Nigerian Research Journal of Chemical Sciences **(ISSN: 2682-6054)**
Volume 10, Issue 1, 2022

Zn(II) Complexes Derived from *ONO* Donor Hydrazone Schiff Base Ligands: Synthesis, Characterization, Antimicrobial and Antioxidant Evaluations

*[1]Waziri, I., [2]Zarma H. A., [1]Fugu M. B., [3]Yesufu H. B., [1]Askira N.K., [1]Mala G.A.

[1]Department of Pure and Applied Chemistry, University of Maiduguri, Maiduguri, Nigeria

[2]Department of Biochemistry, University of Maiduguri, Maiduguri, Nigeria

[3]Department of Pharmaceutical Chemistry, University of Maiduguri, Maiduguri, Nigeria

*Corresponding Author: waiziriibrahim@unimaid.edu.ng

ABSTRACT

Herein, Zn(II) complexes derived from halo-substituted hydrazone ligands, (HL1 and HL2), were synthesised and characterized using ^{1}H NMR, ^{13}C{H}NMR, FT-IR, UV-Vis, mass spectroscopy, elemental (CHN)/metal content analyses, thermal analysis (TGA), SEM-EDX and conductivity measurement. The IR spectral data showed that both ligands acted as tridentate and coordinated to the Zn(II) ion through carbonyl group (C=O), oxygen atom of the hydroxyl group (O-H), and the nitrogen atom of the azomethine (HC=N), whereas the fourth bond that occurred via oxygen atom of the water molecule completed the tetrahedron geometry. The antimicrobial potentials of the compounds were evaluated using disc diffusion method, on some selected bacteria: *Bacillus subtilis* (Bs) and *Staphylococcus aureus* (Sa) (Gram-positive) and *Klebsiella pneumonioe* (Kb) and *Escherichia coli* (Ea) (Gram-negative). From the results obtained, the complexes were more potent than their free ligands with [ZnL2(H_2O)] displaying enhanced activity compared with [ZnL1(H_2O)]. In addition, the radical scavenging ability of the compounds was evaluated using (DPPH, ABTS$^{\bullet}$, $^{\bullet}$OH and $O_2^{-\bullet}$ radicals). This result shows that the ligands demonstrated less *in vitro* antioxidant activity on all the free radicals than their complexes, in which [ZnL2(H_2O)] complex displayed enhanced antioxidant activity than [ZnL1(H_2O)]. The antioxidant activity result obtained showed similar trend with that of antimicrobial study.

Keywords: Biological application, Hydrazone, Metal complexes, Salicylaldehyde, Schiff bases.

INTRODUCTION

Schiff bases have gained recognition as one of the frontline ligands in the field of coordination chemistry due to their stability, flexibility toward coordination, ease of synthesis and structural diversity. These ligands are good chelating agents toward transition and main group metals [1-5].

In recent time, Schiff bases derived from hydrazide with aldehydes or ketones (hydrazones) are gaining more attention due to their versatility [6-10]. Hydrazones (Figure 1) are class of compounds containing RC=NNH group and they are obtained via condensation of hydrazine with aldehydes or ketones [11-13].

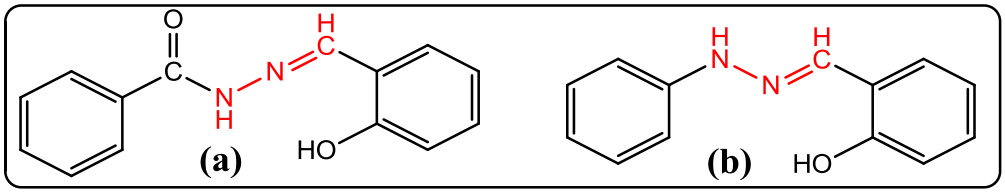

Figure 1: Hydrazones derived from (a) Salicylaldehyde with benzohydrazide and (b). Phenyl hydrazine

Hydrazones derived from benzohydrazide and it derivatives can exist in either keto or enol form (Figure 2), and this gave them ability to coordinate to divalent metals in 1:1 or 1:2 mole ratio for keto and enol forms respectively.

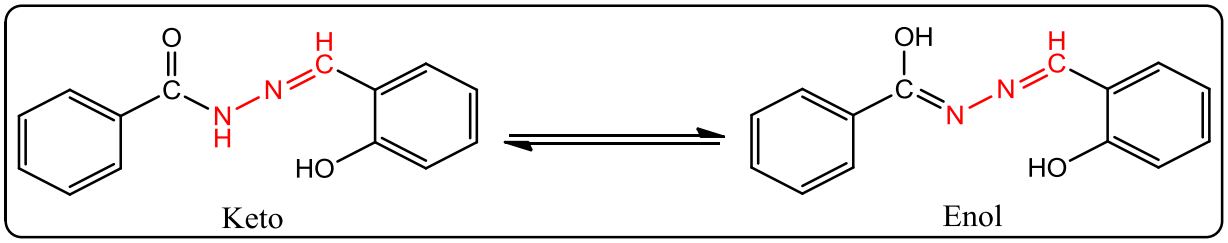

Figure 2: The presentation of keto and enol forms of hydrazone derived from salicylaldehyde and benzohydrazide

The chemistry of these compounds, especially those containing oxygen and nitrogen donor atom together with their metal complexes are receiving attention owing to their fascinating biological properties [14-18]. Hydrazone ligand systems have the ability to form stable metal complexes with different structural diversity and application in various fields such as analytical chemistry, electrochemistry, corrosion inhibition, spectroscopy and medicinal [19-21].

Recently, several researchers reported the scavenging potentials of hydrazone ligands and their metal complexes [8, 22-26] and most of these studies revealed the promising activity demonstrated by the compounds. In addition, the antimicrobial and antifungal potentials of these ligand and their metal complexes were reported by different researchers [9, 27-29]. Similarly, chemotherapeutic ability of hydrazones and its derivatives in the management of tuberculosis is well documented [30-32].

Inspired by the fascinating biological properties of hydrazone ligands and their metal complexes, and in our quest for determining metal complexes of biological importance, we hereby report synthesis of two *ONO* donor halo-substituted hydrazone ligands (HL1 and HL2) and their Zn(II) complexes, and study the influence of halo substituent to the structural and biological properties of the compounds. This is because halogens-containing compounds are known to have biological properties. The incorporation of halogens such as Cl, Br, I and F within a molecules, lead to increased lipophilicity and enhancement of biological activity/lipid membrane penetrations [33]. Similarly, structural activity relationship showed that halogen group increases biological activity of a molecules [33]. These properties are responsible for the remarkable biological activity demonstrated by *N*-(3,5-dichloro-2-hydroxybenzlidene)-4-amino benzene sulfonic acid sodium salt [34]. The choice of zinc ion for this complexation is due to its role in biological system and also its ability to demonstrate unique biological activity when coordinated to low molecular weight ligands. Zinc complexes having lower molecular weight have been involved in various biological process ranging from cellular to metabolic process activities [35].

The hydrazone ligands reported herein were synthesised via condensation of dichloro and dibromo substituted salicylaldehyde with benzohydrazide in methanol as solvent at room temperature. To the best of our knowledge and after literature search, these ligands have not been complexed with Zn(II) ion. However, various researchers had reported the biological study on the free ligands, their Cu(II) complexes and all reported remarkable activities demonstrated by the compounds [36-40].

MATERIALS AND METHODS

The reagents deployed in this research are analytical grade (AR) and purchased from Merck. These reagents were used without any purification unless otherwise stated. They include: 3,5-dichlorosalicylaldehyde, 3,5-dibromosalicylaldehyde, zinc acetate dihydrate, methanol, ethanol, diethyl ether, ethyl acetate, chloroform, dichloromethane, hexane, dimethyl sulfoxide, dimethylformamide, acetone and tetrahydrofuran.

General procedure for the synthesis of the ligands (HL1 and HL2)

The Schiff base ligands HL1 and HL2 were synthesised according to modified literature procedures [41-44]. A solution of 3,5-dichlorosalicylaldehyde (5.0 mol, 0.955 g, 1eq) and of 3,5-bromosalicylaldehyde (5.0 mol, 1.400 g, 1eq) in 30 mL of methanol was reacted separately with

a solution of benzohydrazide (5.0 mol, 0.681 g, 1eq) in 20 mL of methanol. Catalytic amount of formic acid (three drops) was added and stirred at room temperature for 4 h. The resulting precipitate was filtered, washed with methanol, followed by ether and dried over $CaCl_2$ in a desiccator.

_N_'-(3,5-dichloro-2-hydroxybenzylidene) benzohydrazide (HL1)

Yield: 71% (1.4321 g); white powder; m.p. 186-189 ˚C; ^{1}H NMR (500 MHz, DMSO-d_6) δ: (ppm) = 7.56 (t, 2H, Ar-H, *J* = 7.5 Hz), 7.63-7.66 (m, 2H, Ar-H, *J* = 7.0 Hz), 7.68 (d, 1H, Ar-H, *J* = 7.0 Hz), 7.96 (d, 2H, Ar-H, *J* = 7.5 Hz), 8.58 (s, 1H, HC=N), 12.50 (s, 1H, OH), 12.52 (s, 1H, NH); ^{13}C{H}NMR (125 MHz, DMSO-d_6) δ: (ppm) = 162.9 (C=O), 152.2 (C-OH, Ar-C), 146.9 (HC=N), 132. 2, 132.1, 130.1, 128.5 (2C), 128.3 (2C), 127.7, 122.8, 121.4, 120.7 (Ar-C); Selected IR_{ATR}; (υ, cm^{-1}): 3221 (N-H), 3041 (OH), 1652 (HC=N), 1600 (C=O), 1343 (C-N), 706 (C-Cl); UV-Visible (DMSO, 10^{-3} M); 280, 350 nm; CHN Anal. Calculated for $C_{14}H_{10}Cl_2N_2O_2$; C, 54.39; H, 3.26; N, 9.06; found: C, 54.28; H, 3.22; N, 9.04; HRMS-ESI *m/z* $[M+Na]^+$ 331.0060 (Calculated for $C_{14}H_{10}Cl_2N_2O_2$, 331.0017).

_N_'-(3,5-dibromo-2-hydroxybenzylidene) benzohydrazide (HL2)

Yield: 63% (1.6231 g); white powder; m.p. 182-185 ˚C; ^{1}H NMR (500 MHz, DMSO-d_6) δ: (ppm) =7.56 (t, 2H, Ar-H, *J* = 7.5 Hz), 7.64 (t, 1H, Ar-H, *J* = 7.0 Hz), 7.83 (d, 2H, Ar-H, *J* = 7.5 Hz), 7.96 (d, 2H, Ar-H, *J* = 7.5 Hz), 8.54 (s, 1H, HC=N), 12.54 (s, 1H, OH), 12.74 (s, 1H, NH); ^{13}C{H}NMR (125 MHz, DMSO-d_6) δ: (ppm) = 163.0 (C=O), 153.6 (C-OH, Ar-C), 147.0 (HC=N), 135.4, 132.2, 132.1, 132.0, 128.5 (2C), 127.7 (2C), 120.9, 111.1, 110.2 (Ar-C); Selected IR_{ATR}: (υ, cm^{-1}): 3219 (N-H), 3047 (OH), 1655 (HC=N), 1600 (C=O), 1343 (C-N), 869 (C-Br); UV-Visible (DMSO, 10^{-3}M): 310, 380 nm; CHN Anal. Calculated for $C_{14}H_{10}Br_2N_2O_2$; C, 42.24; H, 2.53; N, 7.04; found: C, 42.18, H, 2.49; N, 7.01; HRMS-ESI *m/z* $[M]^+$ 398.2719 (Calculated for $C_{14}H_{10}Br_2N_2O_2$, 398.0494).

General procedure for the synthesis of the metal complexes

The complexes were synthesized following a modified literature procedures [45-47]. Solutions of HL1 (1 mmol, 0.3092 g, 1eq) and HL2 (1 mmol, 0.3981 g, 1eq) in 20 mL of dichloromethane in a separate flask was mixed with a solution of $[Zn(AOc)_2.2H_2O]$ (1 mmol, 0.2195 g, 1eq) in 10 mL of methanol. The solution mixtures were stirred at room temperature for 3 h, the precipitate

formed (complexes) were filtered, washed with methanol, followed by ether and dried in vacuo under P_2O_5 and analysed using various characterization techniques.

[ZnL1(H_2O)]

Yield: 0.1013g (84% based on Zn); yellow solid; m.p. 264-266 ˚C; ^{1}H NMR (500 MHz, DMSO-d_6) δ: (ppm) = 7.28-7.32 (m, 1H, Ar-H, *J* = 7.0 Hz), 7.38 (d, 1H, Ar-H, *J* = 7.0 Hz), 7.41 (d, 3H, Ar-H, *J* = 8.5 Hz), 8.05 (d, 2H, Ar-H, *J* = 7.0 Hz), 8.56 (s, 1H, HC=N); ^{13}C{H}NMR (125 MHz, DMSO-d_6) δ: (ppm) = 169.5 (C=O), 161.8 (C-OH, Ar-C), 152.9 (HC=N), 136.3, 130.6, 129.7, 129.1, 128.6, 127.7, 127.2, 127.1, 125.30, 120.8, 114.4, (Ar-C) Selected IR_{ATR}: (υ, cm^{-1}): 3300 (OH-water), 1604 (HC=N), 1535 (C=O), 1441 (C-N), 848 (C-Cl), 617 (Zn-O), 524 (Zn-N); UV-Visible (DMSO, 10^{-3}M): 354, 446 nm; CHN Anal. Calculated for $C_{14}H_{10}Cl_2N_2O_3Zn$; C, 43.06; H, 2.58; N, 7.17; found: C, 43.04, H, 2.56; N, 7.15; HRMS-ESI *m/z* $[M-H]^-$ 389.8622 (Calculated for $C_{14}H_{10}Cl_2N_2O_3Zn$, 390.5268)

[ZnL2(H_2O)]

Yield: 0.1234 g, (73.5%, based on Zn); dark yellow solid; m.p. 272-274 ˚C; ^{1}H NMR (500 MHz, DMSO-d_6) δ: (ppm) = 7.39 (t, 2H, Ar-H, *J* = 7.5 Hz), 7.41 (d, 2H, Ar-H, *J* = 7.5 Hz), 7.53 (d, 1H, Ar-H, *J* = 7.5 Hz), 8.04 (t, 2H, Ar-H, *J* = 7.0 Hz), 8.51 (s, 1H, HC=N); ^{13}C{H}NMR (125 MHz, DMSO-d_6) δ: (ppm) = 169.5 (C=O), 162.8 (C-OH, Ar-C), 152.5 (HC=N), 136.5, 134.3, 129.6, 127.6 (2C), 127.2 (2C), 121.6, 117.0, 101.4 (Ar-C); Selected IR_{ATR}: (υ, cm^{-1}): 3278 (OH-water), 1610 (HC=N), 1550 (C=O), 1419 (C-N), 802 (C-Br), 617 (Zn-O), 485 (Zn-N); UV-Visible (DMSO, 10^{-3}M): 364, 448 nm; CHN Anal. Calculated for $C_{14}H_{10}Br_2N_2O_3Zn$; C, 35.07; H, 2.10; N, 5.84; found: C, 35.04, H, 2.06; N, 5.78; HRMS-ESI *m/z* $[M-H]^-$ 478.8832 (Calculated for $C_{14}H_{10}Br_2N_2O_3Zn$, 478.4288)

Measurements

The synthesised compounds were subjected to spectroscopic and other analyses to confirm their formation. These include ^{1}H NMR, ^{13}C{H}NMR, FTIR, UV-Visible, Thermogravimetric analysis (TGA), High resolution mass spectroscopy (HRMS), Elemental-CHN analysis and SEM-EDX. The ^{1}H and ^{13}C{H}NMR spectra were recorded on Bruker 500 MHz and 125 MHz, respectively. The Infrared spectral data were obtained using Tensor 27 Bruker and Perking Elmer FT-IR spectrometer BX. The elemental content (CHN) of the ligand and their complexes was obtained using VarioElementar III microbe CHN analyser. All NMR analyses were conducted at

room temperature, and the chemical shifts are reported as parts per million (ppm) relative to tetra methyl silane which is used as internal standards for ^{1}H NMR and $^{13}C\{H\}$NMR in DMSO-d_6.

High resolution mass spectra (HRMS) were carried out on a WatersAcquity UPLC Synapt G2 HD mass spectrometer. Thermogravimetric analyses (TGA) were carried out on a TGA-Q600 thermoanalyzer with a heating rate of 10 $^{\circ}C$ min^{-1} under N_2 flow (20 $mL.min^{-1}$) from room temperature to 800 $^{\circ}C$. The metal content in the complexes were determined using a spectro Arco FSH12 inductively-coupled plasma mass spectrometer.

In vitro antimicrobial study

The synthesized complexes and their free ligands were screened for their anti-microbial activity on Gram-positive (*Staphylococcus aureus* ATCC-25923 (Sa), *Bacillus subtilis* ATCC-6633 (Ba), Gram-negative (*Escherichia coli* ATCC-25922 (Ea), and *Klebsiella pneumoniae* ATCC-13883 (Kp)), using disc diffusion method in DMSO as a solvent at concentrations of 5 and 10 mg/mL [48, 49]. Ciprofloxacin was used as control drug. The zone of inhibition for each of the compound against the tested organisms was measured in triplicate, and the average is presented as mean ± SD.

Determination of minimum inhibitory concentration (MIC)

The MIC of the ligands and their complexes were evaluated using both micro dilution methods [50-52]. The test compounds and control drugs were dissolved in DMSO to obtain the stock and thereafter, it was serially diluted twofold using Mueller-Hinton Broth (MHB) to obtain a concentration range of 512 to 0.25 $\mu g.mL^{-1}$. From the stock solution, 100µL of each concentration was introduced into a well (96well micro plate) containing 90 µL of MHB, followed by the addition of 10 µL of inoculums (1×106 $CFU.mL^{-1}$) of the bacteria to obtain a final concentration range of 250 to 0.125 $\mu g.mL^{-1}$. After which, plates were covered and incubated on a shaker at 37 °C for 24 h. MICs were assessed visually after the corresponding incubation period and were taken as the lowest sample concentration at which there was no growth. Ciprofloxacin was used as positive controls, while broth with 20 µL of DMSO was used as a negative control to determine its influence on the biological systems. This is because it was present as a carrier for the compounds to assist in their solubilisation. The assay was repeated thrice.

Antioxidant assay

DPPH radical scavenging activity

Radical scavenging ability of the free ligands and their complexes was assessed using 1,1-diphenyl-2-picrylhydrazyl (DPPH) radical. The method reported by some researchers was adopted with some modifications [53, 54]. Exactly, 50 µL solution of the compounds in DMSO at different concentration (10, 20, 50, 100 and 150 $\mu g.mL^{-1}$ was mixed with 200 µL of DPPH in methanol and allowed to react in the dark room for 30 min. The absorbance of the resulting pale yellow mixture was measured using UV-Vis spectrometer at a wavelength 517 nm. Ascorbic acid was used as positive control, and measurements were carried out in triplicate. The scavenging activity of the ligands and their complexes against DPPH radical was evaluated using the relation as follows:

DPPH radical scavenging activity (%) =$[((A_0-A_1/A_0)\ X\ 100]$

Where A_0 = absorbance of control (blank solution), and A_1 = absorbance of the sample.

ABTS$^{\bullet}$ free-radical scavenging activity

The ABTS$^{\bullet}$ assay was conducted using a modified literature procedure [55-57]. To generate ABTS, oxidation reaction was carried out using potassium per sulfate (2.45 mM) and 7.0 mM of ABTS, and allowed to react overnight. The solution of the ABTS$^{\bullet}$ was further diluted with deionized water, and the absorbance of the diluted solution was recorded at 734 nm. Thereafter, 40 µL of the DMSO solutions of ligands and their complexes using concentration of (5, 10, 20, 30 and 40 $\mu g.L^{-1}$) was added to 200 µL of ABTS$^{\bullet}$ solution, mixed and incubated in a dark room for 15 min. After the incubation period, absorbance of this mixture was measured at 734 nm using UV-Vis and ascorbic acid was used as positive control. The measurements were carried out in triplicate and the ABTS$^{\bullet}$ radical scavenging activity was estimated using the relation:

ABTS$^{\bullet}$ radical scavenging activity (%) = $[((A_0-A_1/A_0)\ X\ 100]$

Where A_0 = absorbance of control (blank solution), and A_1 = absorbance of the sample.

Hydroxy free-radical ($^{\bullet}$OH) scavenging activity

This assay was performed using modified literature procedure [55-57]. 100 µL of ferrous sulphate (18 mM), 5 µL of 0.03 % H_2O_2 and 50 µL of various concentrations (5, 10, 15, 20 and 25 $\mu g.mL^{-1}$) of the ligands and their complexes in DMSO were thoroughly mixed and incubated

at 37 ˚C for 45 min. Thereafter, it was centrifuged at 3000 rpm for 25 min, and absorbance of the supernatant was recorded using spectrophotometer at 532 nm and compared with reference (ascorbic acid) as positive control. The recording was done three times, and $^{\bullet}OH$ radical scavenging activity was estimated using the relation:

$^{\bullet}OH$ radical scavenging activity (%) = $[((A_0-A_1/A_0) \times 100]$

Where A_0 = absorbance of control (blank solution), and A_1 = absorbance of the sample.

Superoxide anion radical ($O_2^{-\bullet}$) scavenging activity

A literature procedure was adopted for this assay [55-57]. Exactly,2 mL of various concentration (5, 10, 15, 20 and 25 µg.mL^{-1}) of the ligands and their complexes in DMSO, 5 mL of Tris-buffer (50 mmol, pH = 8.2), and 1 mL of benezen-1,2,3-triol solution (0.01 mol.L^{-1} HCl) were added and allowed to react for 10 min at 25 ˚C. The reaction was quenched with 1 mL of HCl (0.008 mmol.L^{-1}), and absorbance was measured at 550 nm. Ascorbic acid was used as positive control, and measurement was carried out in triplicate. The superoxide anion scavenging activity was estimated using the relation:

$O_2^{-\bullet}$ superoxide anion radical scavenging activity (%) = $[((A_0-A_1/A_0) \times 100]$

Where A_0 = absorbance of control (blank solution), and A_1 = absorbance of the sample.

Determination of IC_{50}

The IC_{50} value required for 50% of the free radicals scavenging by the compounds were determined from a series of dose-response data (sample concentration and free radicals scavenging (%)). Using an X-Y plot fitted with a linear regression line and the EC_{50} was estimated using the following relationship; IC_{50} (X) = 50 – C/M. Where, C= is the intercept and M= gradient of the line. The IC_{50} values were compared by paired t test. $P< 0.05$ was considered significant. Statistical analysis was performed using SPSS software version 20 and one-way Analysis of variance. Data were presented as Mean ± SEM. from at least three independent experiments (n = 3). Where, $P < 0.05$ is considered statistical significant.

RESULTS AND DISCUSSION

The hydrazone Schiff base ligands HL1 and HL2 were synthesised via classical condensation of 3,5-chlorosalcylaldehyde and 3,5-bromosalicylaldehyde with benzohydrazide in 1:1 mole ratio, using methanol as a solvent (**Scheme 1**).

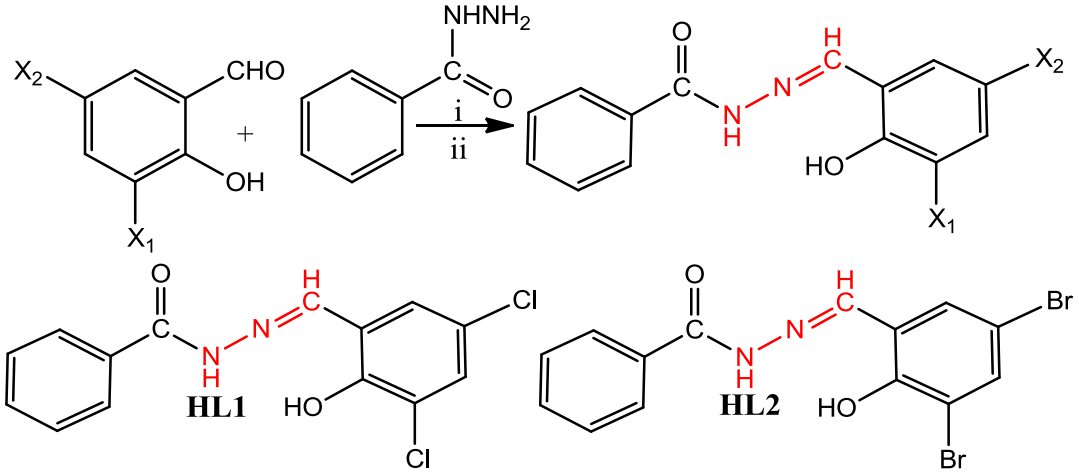

Scheme 1: *Synthesis of the ligands; i = CH_3OH/HCOOH; ii = room temperature*

The Schiff bases were obtained as white powder, air and moisture stable, soluble in polar solvents but insoluble in non-polar solvents. However, the intensity of the colours varies and could be due to the influence of the halo substituents. The metal complexes (Figure 3) were obtained by the reaction of the hydrazone Schiff bases with $Zn(OAc)_2 2H_2O$ in the ratio of 1:1 in a mixture of CH_2Cl_2/CH_3OH at room temperature (Scheme 2). The complexes were obtained in moderate yield as yellow and dark yellow solids; similar variation of color intensity was observed on the complexes. They are soluble in methanol, ethanol, DMSO, DMF and water, but insoluble in chloroform, dichloromethane and non-polar solvents. The solubility of the complexes in polar solvents suggested that they probably polar complexes. The molar conductivity measurement of solution of the complexes in (DMSO, 10^{-3}M) was found to be 8.42 and 9.63 Ω^{-1} cm^2 mol^{-1}, suggesting non-electrolytic complexes. The ligands and their complexes were characterized using ^{1}H NMR, ^{13}C{H}NMR, FTIR, UV-Visible, TGA, HRMS and Elemental analysis. The data obtained from the elemental analysis (CHN) on the ligands and their complexes correlate well with stoichiometric composition of the compounds and are in good agreement with the theoretical values. The physico-chemical and analytical data of the ligands and complexes are presented in Table 1.

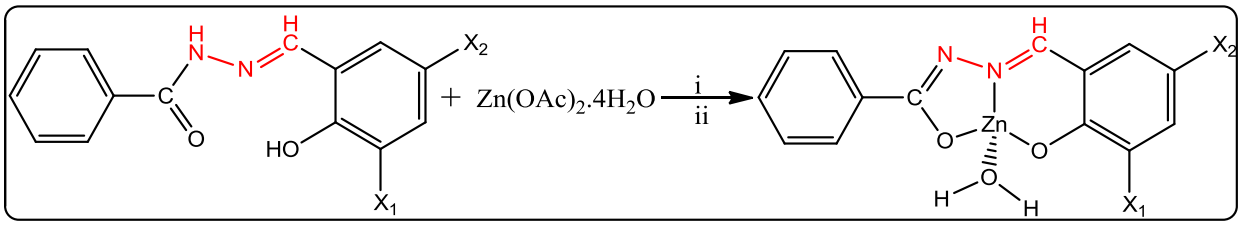

Scheme 2: Synthesis of the complexes i = CH_2Cl_2/CH_3OH; ii = RT; X_1 = X_2 = Cl or Br

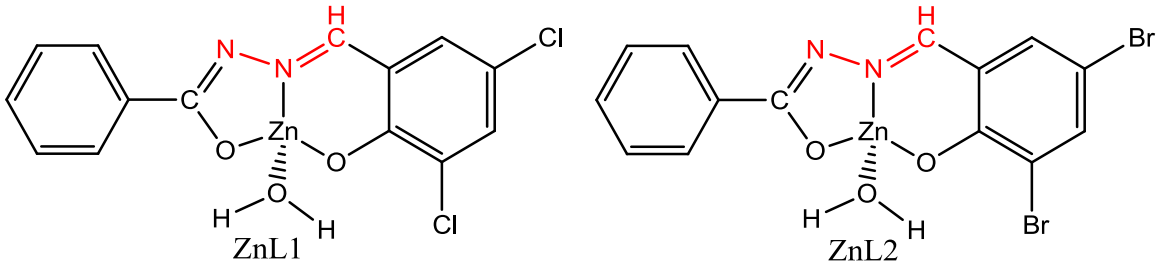

Figure 3: Structure of the complexes

Table 1: Physico-chemical properties of the ligands and their complexes

Compound	Molecular formula (Molecular weight)	Colour	Yield % (g)	m.p./d.p (˚C)	Elemental analysis: Calc. (found)				Molar conductivity ($\Omega^{-1}cm^2mol^{-1}$)
					C	H	N	Zn	
HL1	$C_{14}H_{10}Cl_2N_2O_2$ (309.1474)	White	71 (1.4320)	186-189	54.39 (54.28)	3.26 (3.22)	9.06 (9.04)	-	-
HL2	$C_{14}H_{10}Br_2N_2O_2$ (398.0494)	White	63 (1.6231)	182-185	42.24 (42.18)	2.53 (2.49)	7.04 (7.01)	-	-
[ZnL1(H_2O)]	$C_{14}H_{10}Cl_2N_2O_3Zn$ (390.5268)	Yellow	84 (0.1013)	264-266	43.06 (43.04)	2.58 (2.56)	7.17 (7.1)	16.74 (16.68)	8.42
[ZnL2(H_2O)]	$C_{14}H_{10}Br_2N_2O_3Zn$ (479.4288)	Dark yellow	74 (0.1234)	272-274	35.07 (35.04)	2.10 (2.06)	5.84 5.78)	13.64 (13.61)	9.63

m.p. = Melting point; d.p. = Decomposition point; Calc. = Calculated; g = Grams

^{1}H NMR and ^{13}C{H}NMR spectral study

Nuclear magnetic resonance (NMR) spectroscopy is one of the vital tools that are used in structural elucidation. It is used to ascertain how atoms within a particular molecule are related. This is achieved by analyzing chemical domain of the selected nucleus.

To establish the formation of the compounds and also to elucidate their structure, the ^{1}H NMR and ^{13}C{H}NMR spectra of the ligands and their diamagnetic Zn(II) complexes were recorded in DMSO-d_6 (Figures 4-11). The spectra of both the ligands and their complexes showed different peaks that were characteristics of the compounds. Furthermore, both the spectra of HL1 and HL2 presented peaks in a similar chemical environment due to their structural similarity. A sharp single peak at 12.54 and 12.74 ppm in the ligands is due to the –NH proton of the hydrazide moiety in HL1 and HL2 respectively (Figures 4-5). The appearance of this proton in the downfield region is an indication of its involvement in intra-molecular hydrogen bonding with the carbonyl oxygen of the benzohydrazide. This is because hydrogen bonding often lowered the electron density around the proton, and hence moves the absorption of the proton to the downfield. Similarly, the phenolic protons of ligands were observed at 12.50 and 12.54 ppm as a sharp single peak. These protons appeared in downfield region due to the electronegative effect of oxygen atom, which causes the proton to be de-shielded and subsequently occurred in the downfield region. The azomethine proton (HC=N) signals were observed at 8.54 and 8.58 ppm in the two ligands respectively. This peak appeared upfield compared to the usual azomethine proton in Schiff bases.

Thus, it can be said that the position of these protons is affected by the electronegative character of the substituted halogens on the benzene ring. The chemical shifts of the aromatic protons in both ligands were observed within 7.55 –7.96 ppm. There is also appearance of single sharp peak at 3.31 ppm in all the spectra, which is due to the moisture (water) in the DMSO-d_6 that was used for the NMR (Figures 4-5).

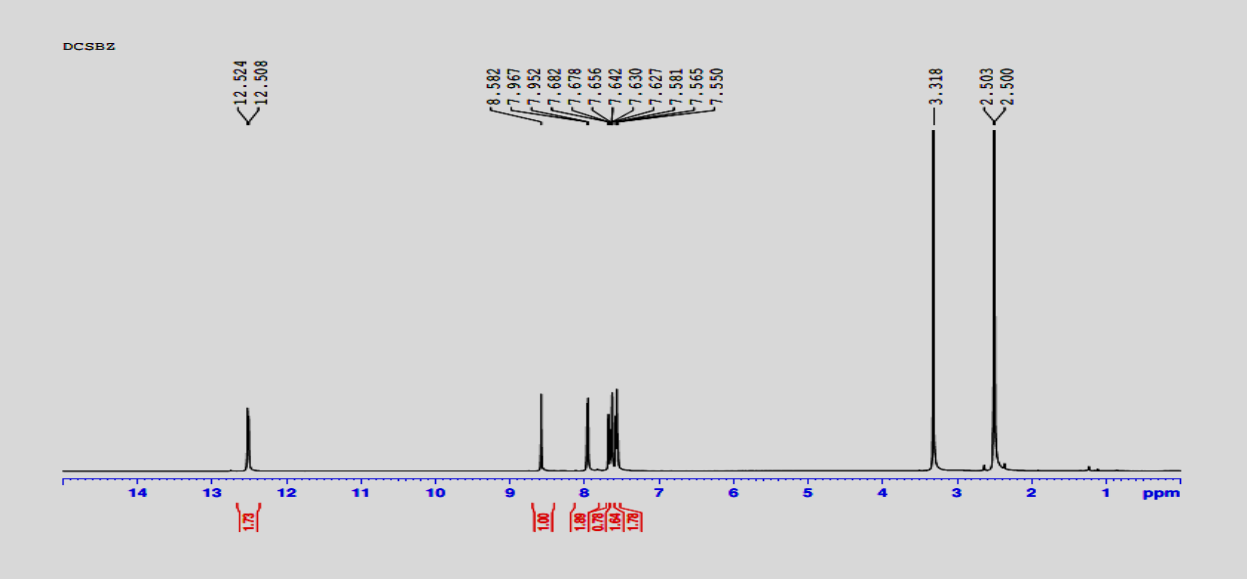

Figure 4: ^{1}H NMR spectrum of HL1, (500 MHz, DMSO-d_6)

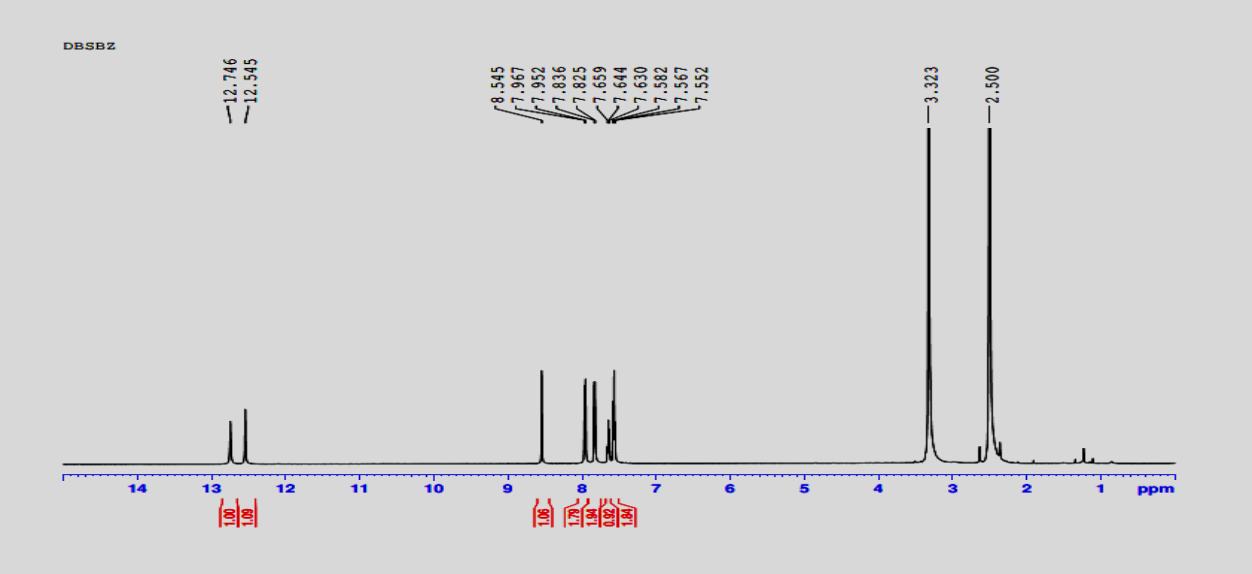

Figure 5: ^{1}H NMR spectrum of HL2, (500 MHz, DMSO-d_6)

The carbonyl (C=O) carbon and the aromatic carbon that is directly linked to the phenolic oxygen (C-OH) were observed in the downfield region at 162 – 163 ppm and 152 – 153.6 ppm respectively (Figures 6-7). In the same manner, the azomethine (HC=N) carbon and the aromatic carbons were obtained around 146 – 147 ppm and 110 – 135.4 ppm in both ligands respectively (Figures 6-7).

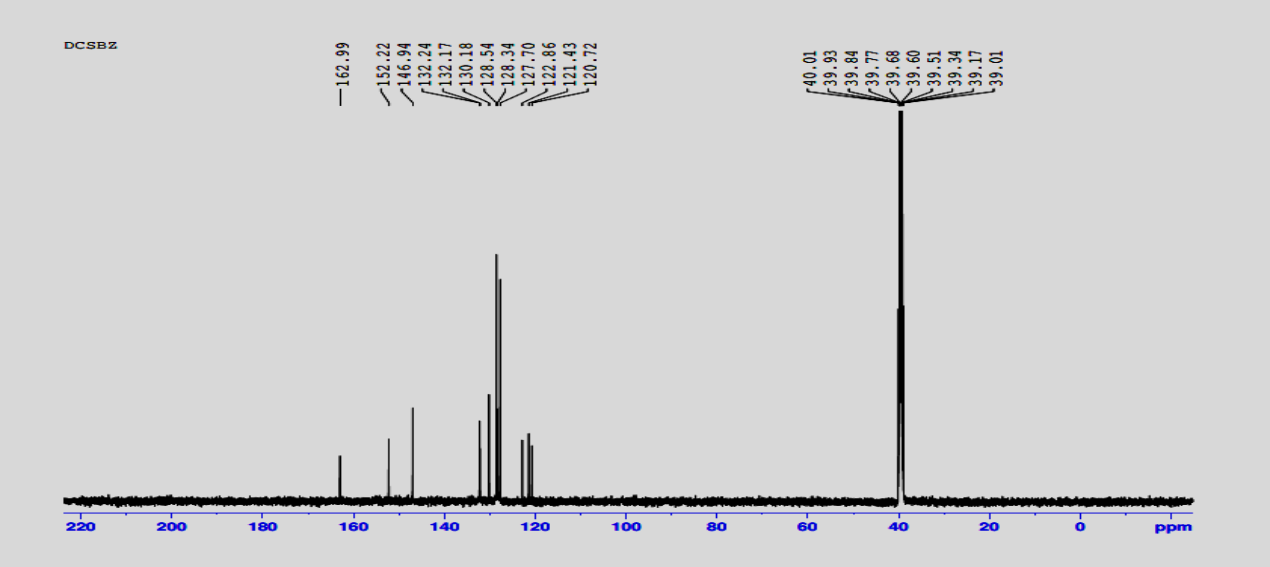

Figure 6: $^{13}C\{H\}$NMR spectrum of HL1, (125 MHz, DMSO-d_6)

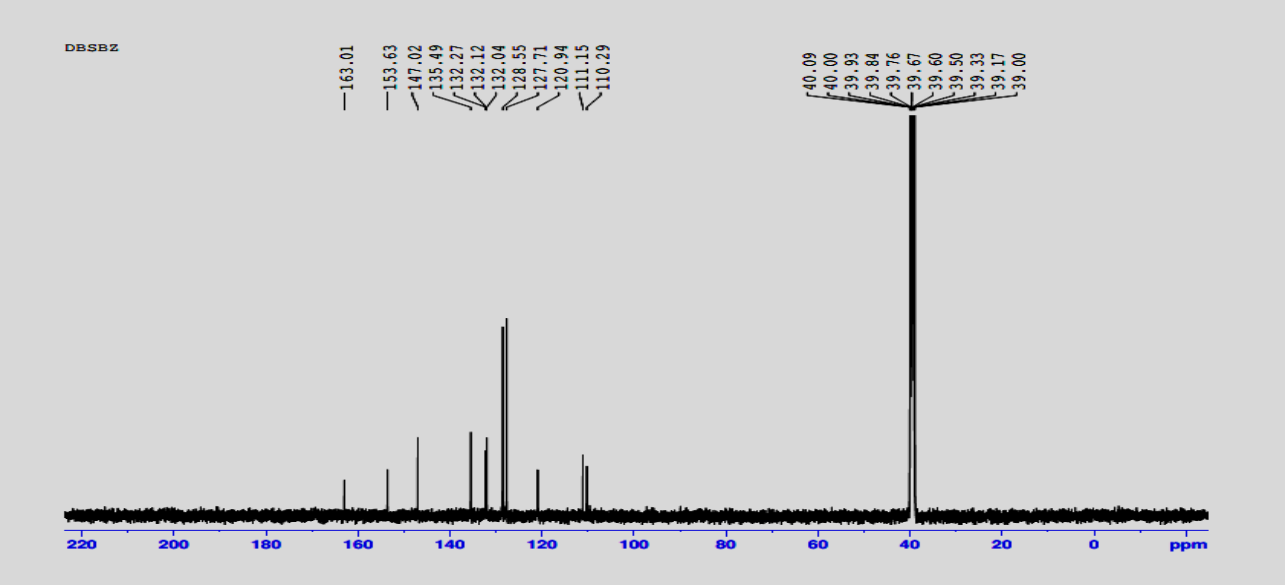

Figure 7: $^{13}C\{H\}$NMR spectrum of HL2, (125 MHz, DMSO-d_6)

After coordination to the Zn(II) ion, and as can be seen from the ^{1}H NMR spectra of the complexes (Figures 8-9).The –NH and –OH protons that appeared downfield in the free ligands did not appear on the spectra of the complexes. The disappearance of these protons in the complexes confirmed the deprotonation of the protons, and coordination of the Zn(II) ion to the ligand through oxygen atom of the hydroxyl and carbonyl groups. Similarly, the deprotonation of the hydrazide proton further affirmed the existence of hydrogen bonding between the hydrazide proton and the carbonyl oxygen. In addition, the azomethine and the aromatic protons were

significantly shifted in the complexes (Figures 8-9). The shift in the chemical environment of the azomethine proton is due to the involvement of the nitrogen atom in the coordination.

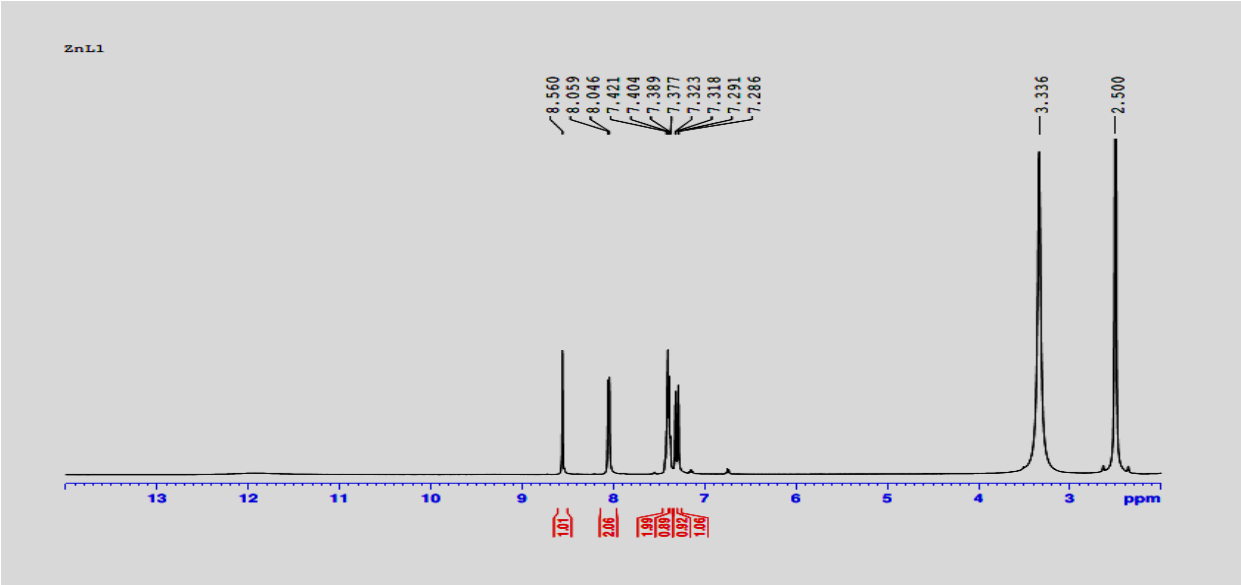

Figure 8: ^{1}H NMR spectrum of [ZnL1(H_2O)], (500 MHz, DMSO-d_6)

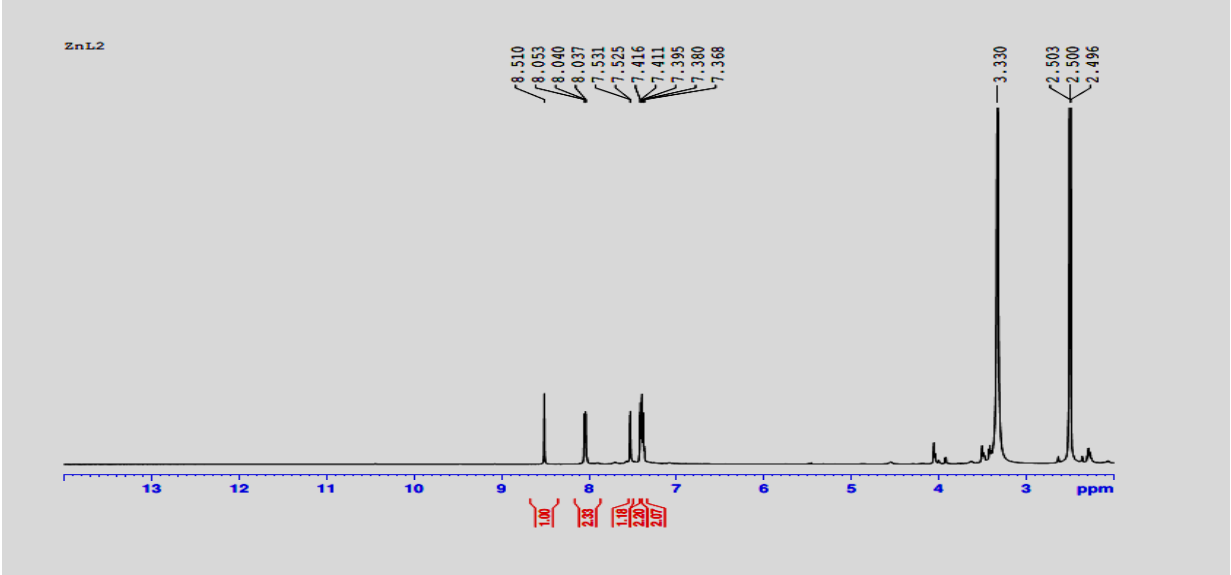

Figure 9: ^{1}H NMR spectrum of [ZnL2(H_2O)], (500 MHz, DMSO-d_6)

The $^{13}C\{H\}$NMR spectra of the complexes (Figures10-11), showed significant shift toward downfield region for (C=O), (C-OH) and (HC=N) carbons. This shifts, confirmed the coordination of the Zn(II) ion through the oxygen and nitrogen atoms of the carbonyl/hydroxyl

and azomethine groups respectively. Also, there is marked shifts in the position of the aromatic carbon owing to the vibration of the molecules due to the complexation.

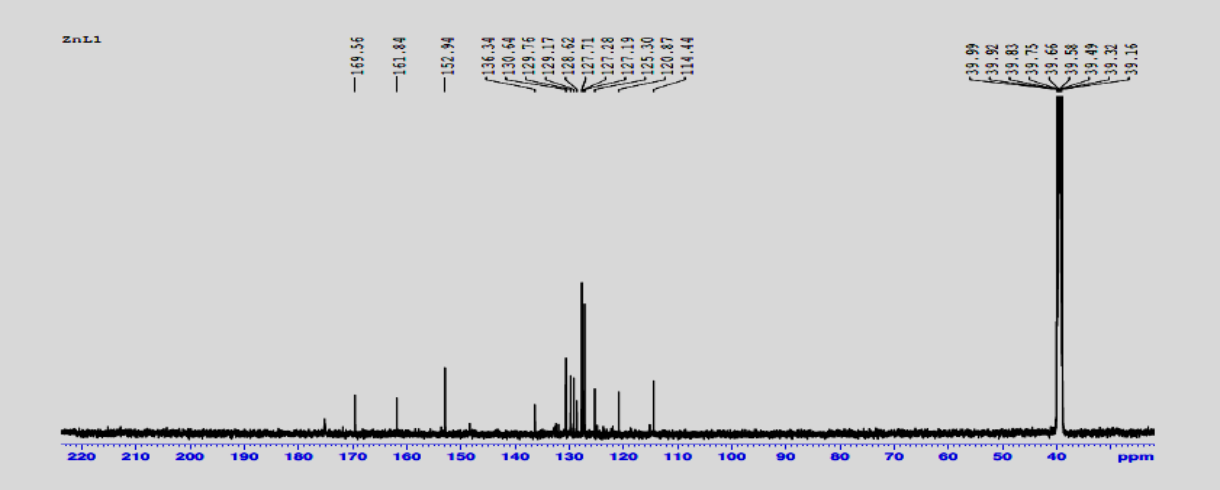

Figure 10: $^{13}C\{H\}$NMR spectrum of [ZnL1(H_2O)], (125 MHz, DMSO-d_6)

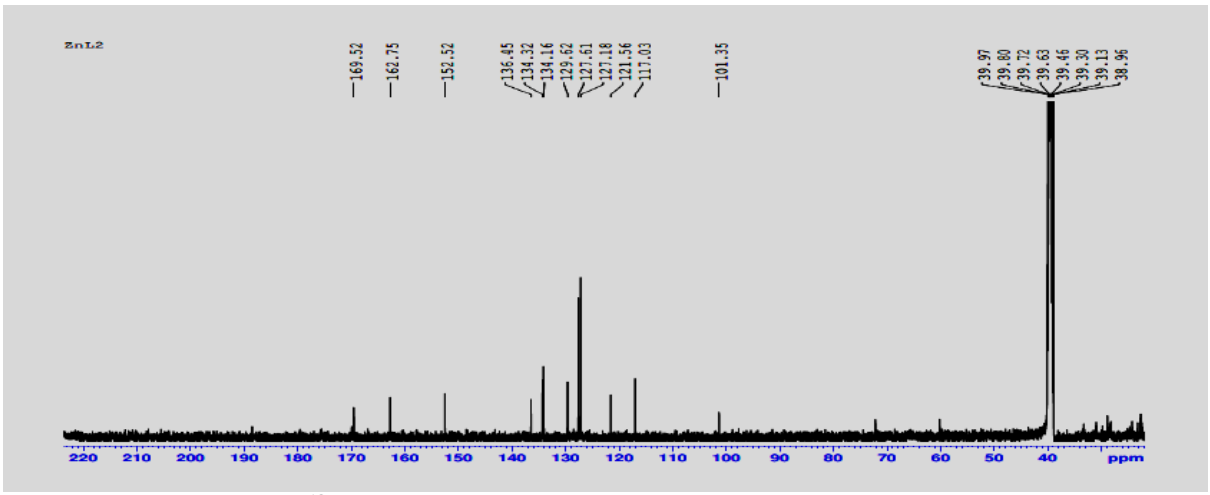

Figure 11: $^{13}C\{H\}$NMR spectrum of [ZnL2(H_2O)], (125 MHz, DMSO-d_6)

Infrared spectra

Infrared spectroscopy plays a vital role in coordination chemistry, and it is one of characterization techniques that are used to confirm the formation of complex between ligands and metal ions. In order to verify the formation of complex, the infrared spectrum of ligand is compared with that of the complex. Herein, the infrared spectra of the ligands and their complexes were obtained in the region of 4000 – 400 cm^{-1}. The data for some selected stretching bands are presented in Table 2, and the spectra are shown in Figure 12.

The spectra of the ligands showed a medium intensity bands at 3221 – 3278 cm^{-1} and 3041 – 3047 cm^{-1}, which are assignable to –NH and –OH characteristic bands for HL1 and HL2

respectively. These bands were not observed on the spectra of the complexes. The disappearance of the bands in the spectra of Zn(II) complexes confirmed the deprotonation of the hydrazide and hydroxyl groups, and coordination of the zinc ion to the ligand via oxygen atom of the carbonyl and hydroxyl groups as seen in the ^{1}H NMR of the complex. The appearance of new band in all the complexes in region of 617 cm^{-1} which are assignable to metal-oxygen band as reported in the literature [58, 59], further confirmed the formation of the complexes.

A stretching band at 1652–1655 cm^{-1} are due to imine (C=N) band of the azomethine moieties within the ligands (Table 2). This band is the key indicator for the formation of Schiff bases [60, 61]. The bands shifted to lower frequency (1604–1610) cm^{-1} on the spectra of the complexes. The shift to the lower frequency upon complexation and subsequent formation of new band at 485–524 cm^{-1} due to metal-nitrogen band, confirmed the involvement of the azomethine nitrogen in the complexation.

Similarly, the carbonyl (C=O) band stretching was observed at 1600 cm^{-1} in both ligands, and bands shifted to 1535–1555 cm^{-1} in the complexes due to the participation of the carbonyl oxygen in the coordination. The –C-N and C-Cl/C-Br stretching vibration frequencies were noted at 1343, 706 and 869 cm^{-1} respectively in the free ligand. The bands were observed at 1419-141, 848 and 802 cm^{-1} in the complexes. The shifts in these bands are as a result of the vibration within the molecules arising from complexation.

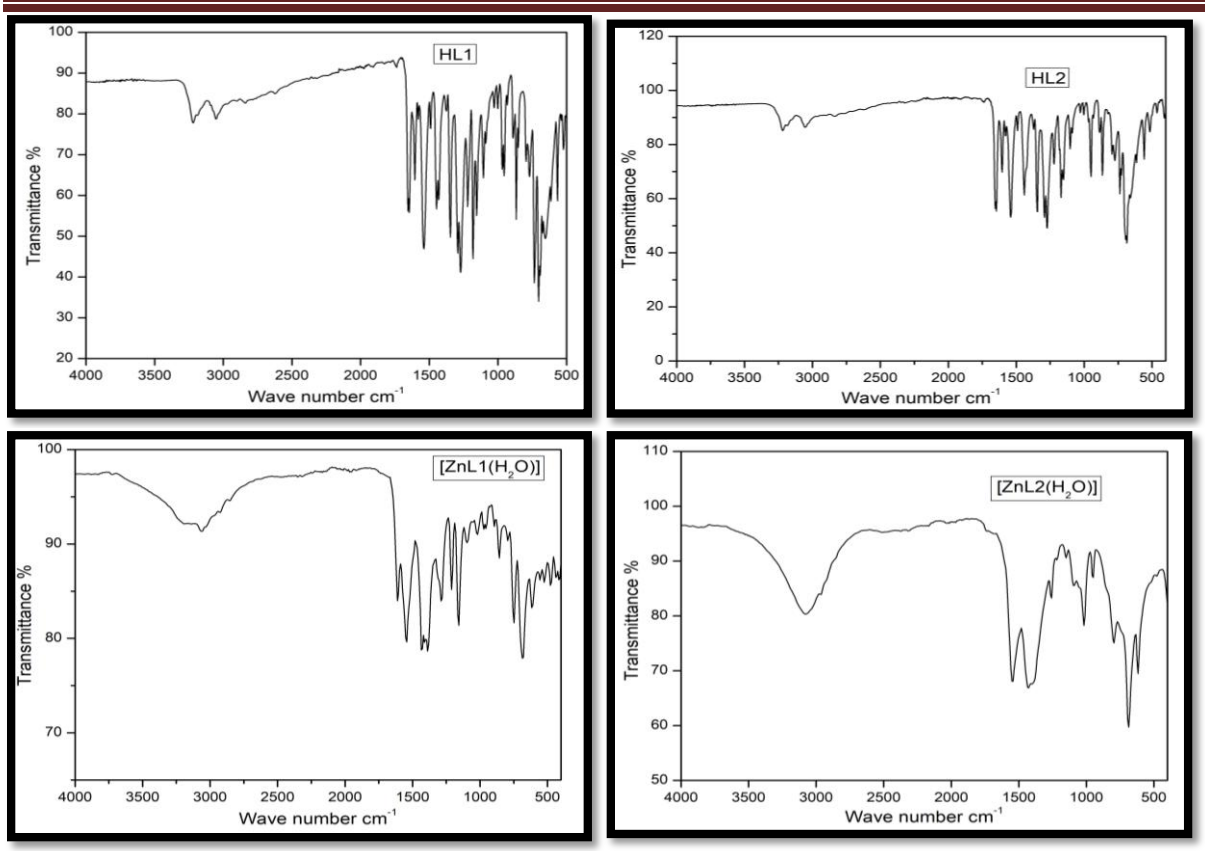

Figure 12: FTIR spectra of the ligands and their complexes

Table 2: Infrared spectral data of the ligands and their complexes

Compounds	**υ(O-H-water)**	**υ(N-H)**	**υ(O-H-phenolic)**	**υ(HC=N)**	**υ(C=O)**	**υ(C-N)**	**υ(C-Cl)**	**υ(C-Br)**	**υ(Zn-O)**	**υ(Zn-N)**
HL1	-	3221	3041	1652	1600	1343	706	-	-	-
HL2	-	3219	3047	1655	1600	1343	-	869	-	-
[ZnL1(H_2O)]	3300	-	-	1604	1535	1441	848	-	617	524
[ZnL2(H_2O)]	3278	-	-	1610	1550	1419	-	802	617	485

Electronic spectral study

To establish the formation of the complexes, electronic spectral study was carried out on the free ligands and their complexes in DMSO (10^{-3}M).The spectra are presented in Figure 13, and summary of the data is shown in Table 3.The spectra of the ligands displayed absorption bands at 292–383 nm and 329–360 nm respectively. These peaks can be attributed to $\pi\rightarrow\pi^*$ and $n\rightarrow\pi^*$ within the aromatic moiety and azomethine group respectively [62]. On complexation, these bands shifted to lower wavelength at 353–447 nm and 370–432 nm respectively. These bands are assignable to charge transfer transition of the type O(pπ)–Zn(dπ) and N(pπ)–Zn(dπ), respectively due to the ON donor ligands system in a tetrahedral geometry[63].Furthermore, Zn(II) complexes with tetrahedral geometry experienced orbital splitting pattern of $dx^2–y^2$ and dz^2 with low orbital energy as the result of the orbital between the ligand axis experiences little repulsion. Therefore, coordination entities such as racah parameters (B), nephelauxetic ratio (β) and crystal field splitting energy (Δ_o) will be very minimal or insignificant.

Table 3: Electronic spectral data of the ligands and their complexes

Compound	λ max (nm)	Band assignment	Geometry
HL1	292	$\pi\rightarrow\pi^*$	–
	383	$n\rightarrow\pi^*$	
HL2	329	$\pi\rightarrow\pi^*$	–
	360	$n\rightarrow\pi^*$	
[ZnL1(H_2O)]	353	$n\rightarrow\pi^*$	Tetrahedral
	447	LMCT	
[ZnL2(H_2O)]	370	$n\rightarrow\pi^*$	Tetrahedral
	432	LMCT	

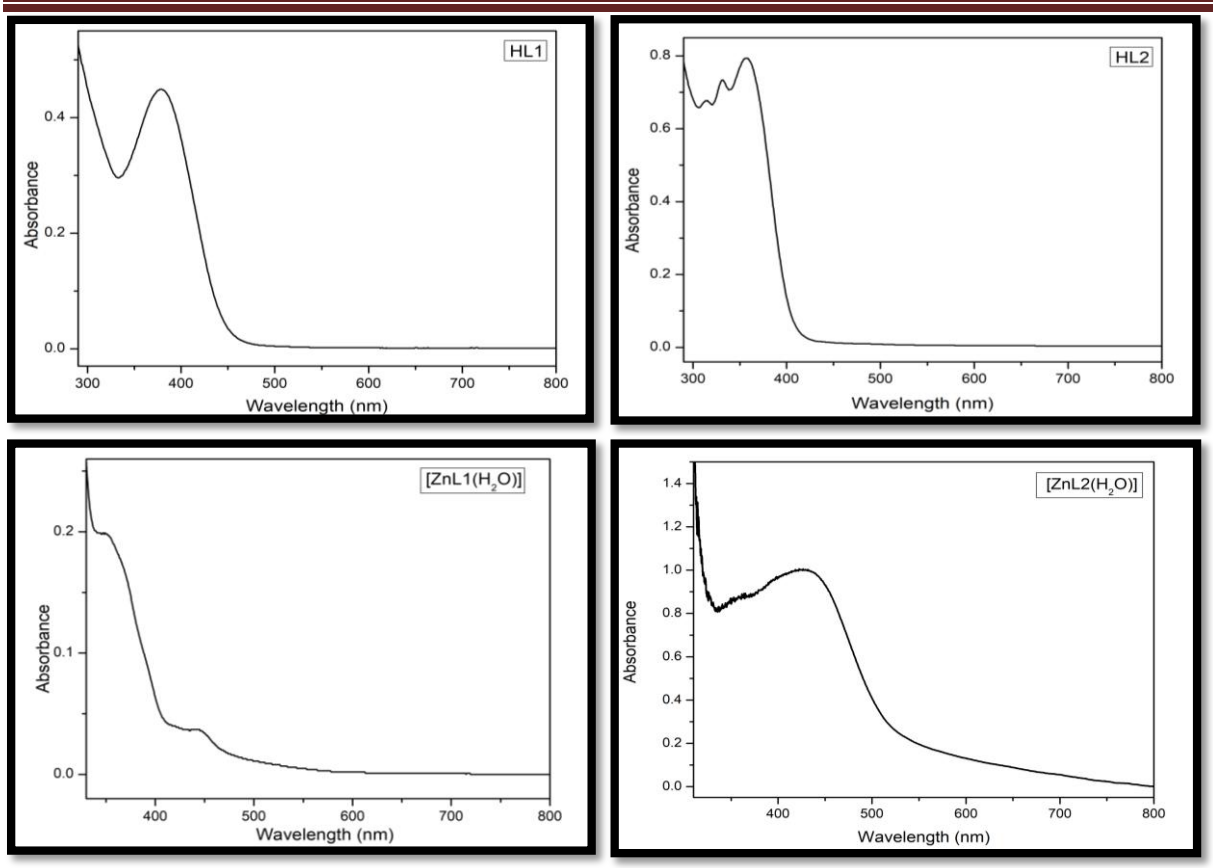

Figure 13: UV-Visible spectra of the ligands and their complexes

Thermal study

To study the thermal stability of the synthesised complexes, thermogravimetric analysis (TGA) was carried under nitrogen at 25–800 ˚C using heating rate of 30 ˚C/min. The thermal behavior of the complexes at this temperature range (Figure14), displayed three decomposition stages. The [ZnL1(H_2O)] showed decomposition at *ca* 25–117 ˚C with a weight loss of 4.11% (calculated as 4.6%), [ZnL1(H_2O)] had first decomposition at 25–115 ˚C with loss of 3.68% (calculated as 3.77%). These weight loses correspond to one molecular of water. The second decomposition stages were observed at *ca* 120–420 ˚C and 120–338 ˚C on the thermograms of the complexes respectively, with a weight loss of 79.20% and 79.42% (calculated as 81.45 % and 83.0%). These decompositions could be assigned to the loss of organic molecules (ligands) within the complexes. The third decomposition stages represent decomposition of the zinc ion with subsequent formation of ZnO respectively. From this result of the thermal behavior of the complexes, it could be deduced that the chloro and bromo substituent did not cause significant difference to the thermal stability of the complexes.

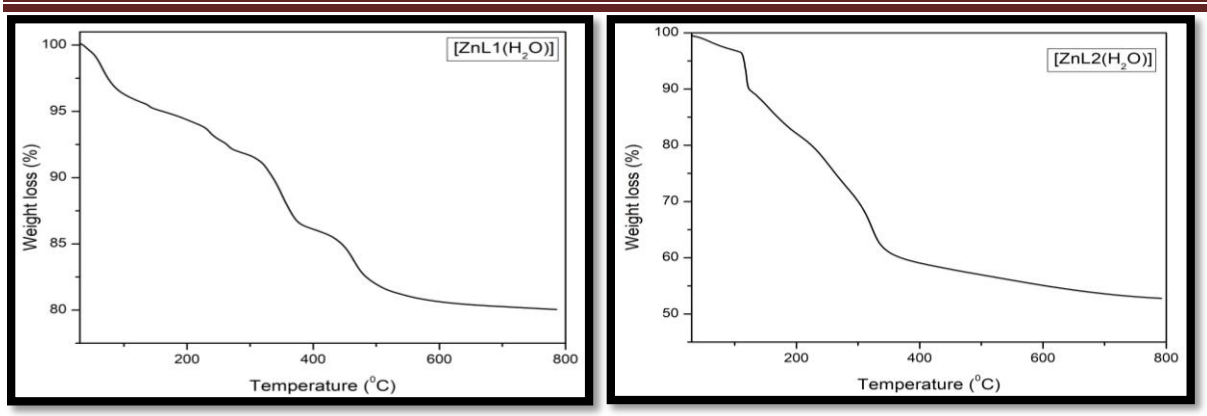

Figure 14: Thermograms of the complexes

ESI-mass spectral study

The mass spectra of the ligands and their complexes (Figures 15–18) were obtained and the molecular ion peaks confirm the molecular structures of the compounds. The spectrum of HL1 shows molecular ion peak at *m/z* = 331.0060 corresponding to $[M+Na]^+$ ion. In addition, the spectrum displayed *m/z* = 330.0032 and 176.994 representing various fragments of the HL1 molecule. The spectrum of HL2 exhibits peak at *m/z* = 398.2719 corresponding to $[M]^+$ ion. Furthermore, *m/z* = 274. 2937 was also observed on the spectrum and this corresponds to $C_7H_4Br_2NO^*$ fragment of HL2 molecule. The spectra of the complexes confirmed the proposed structures of the complexes. The spectrum of $[ZnL1(H_2O)]$ showed peak at *m/z* = 389.8662 which correspond to $[M-H]^-$ based on the proposed structure (Figure3). The peaks at 320.9141, 225.9308, and 149.9172 represent different fragments of the complex, respectively. Similarly, the spectrum of $[ZnL2(H_2O)]$ showed peak at *m/z* = 478.8832. This corresponds to $[M-H]^-$ confirming the proposed structure (Figure 3). Other fragments of the complex were observed on the spectrum, and these include 475.8803, 474.880, 463.8939 and 291.8918 respectively.

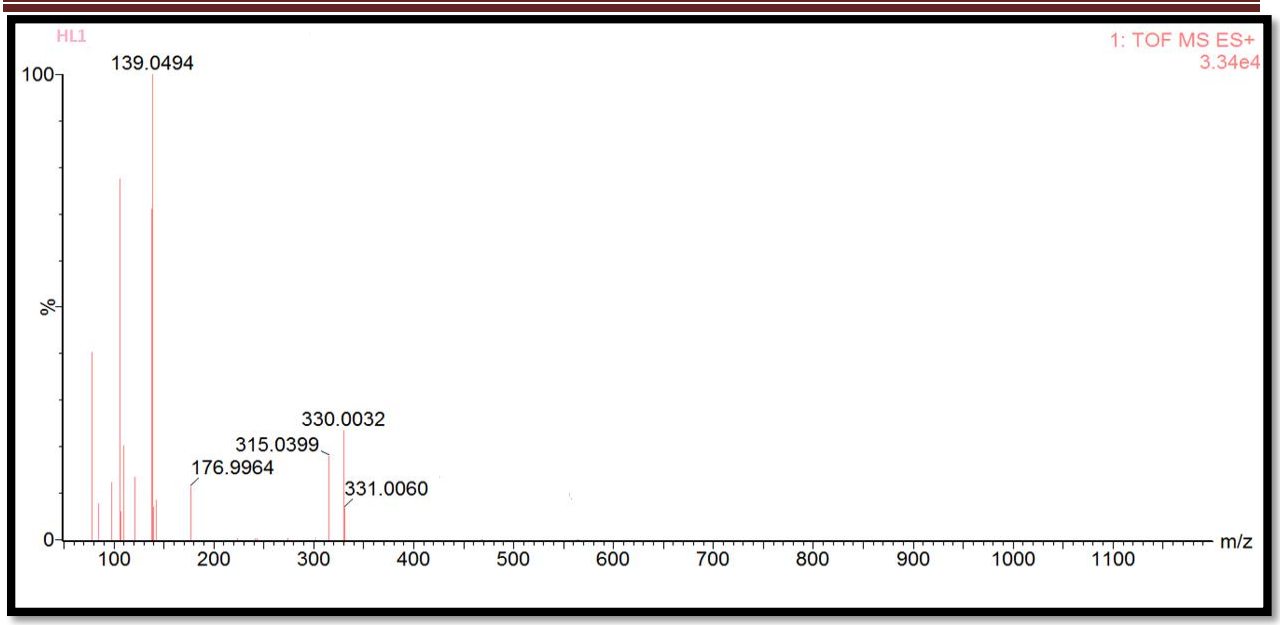

Figure 15: Mass spectrum of HL1 ligand

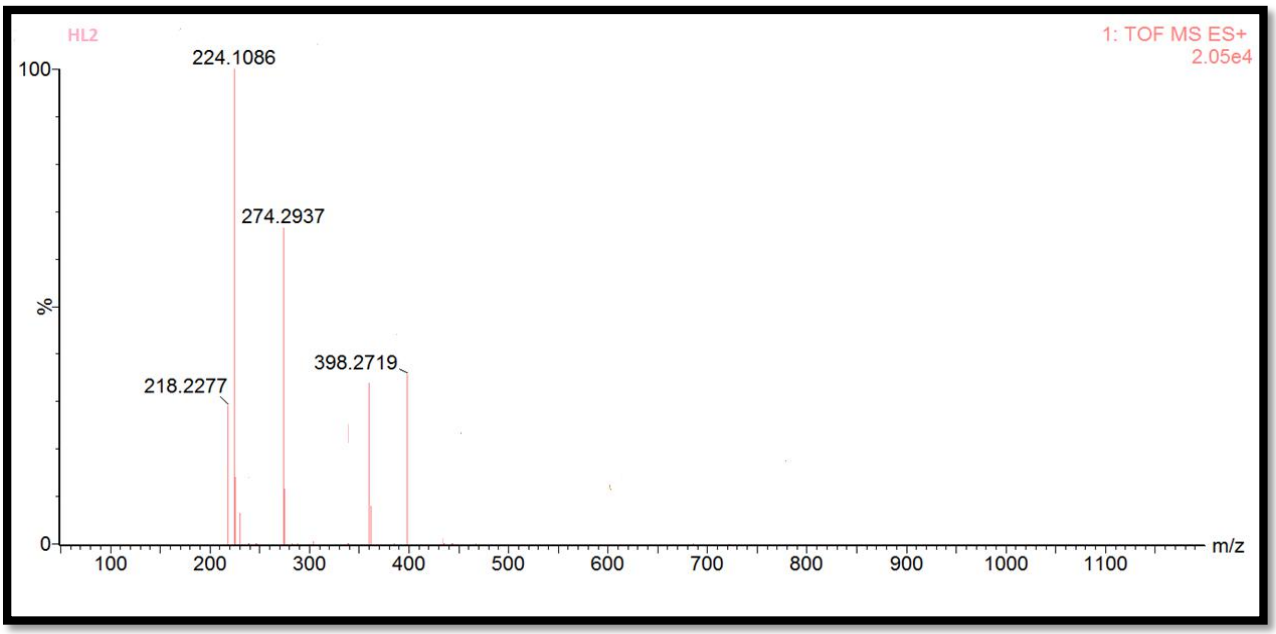

Figure 16: Mass spectrum of HL2 ligand

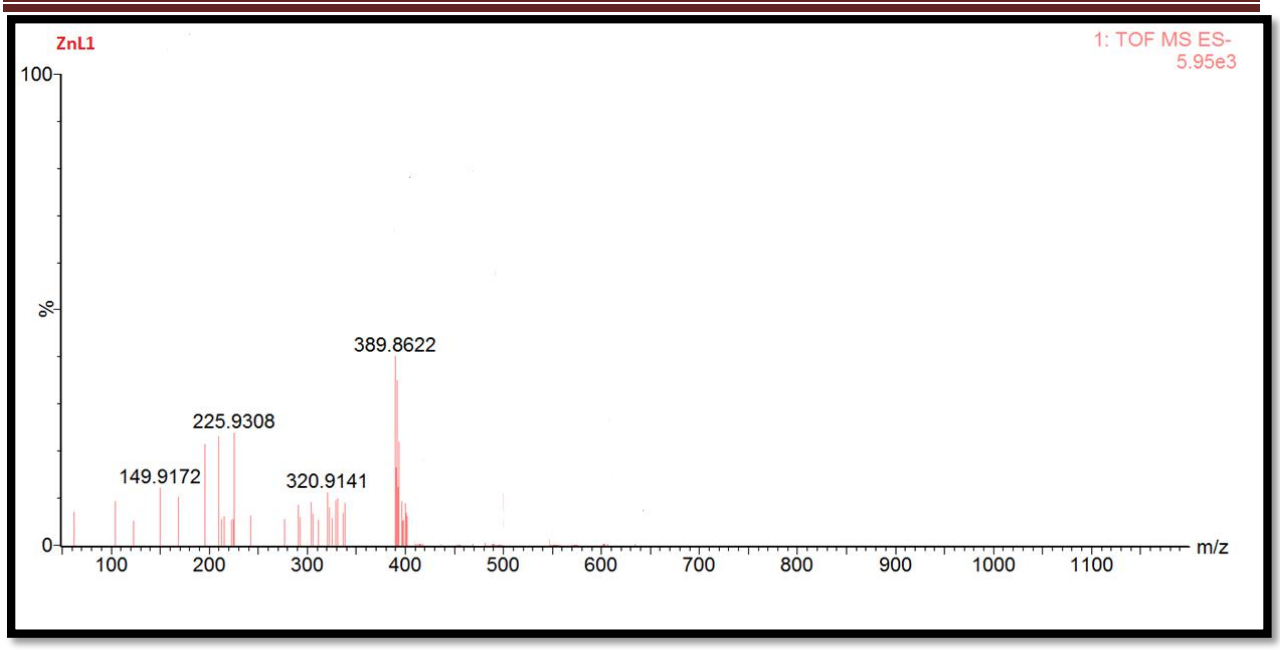

Figure 17: Mass spectrum of [ZnL1(H_2O)] complex

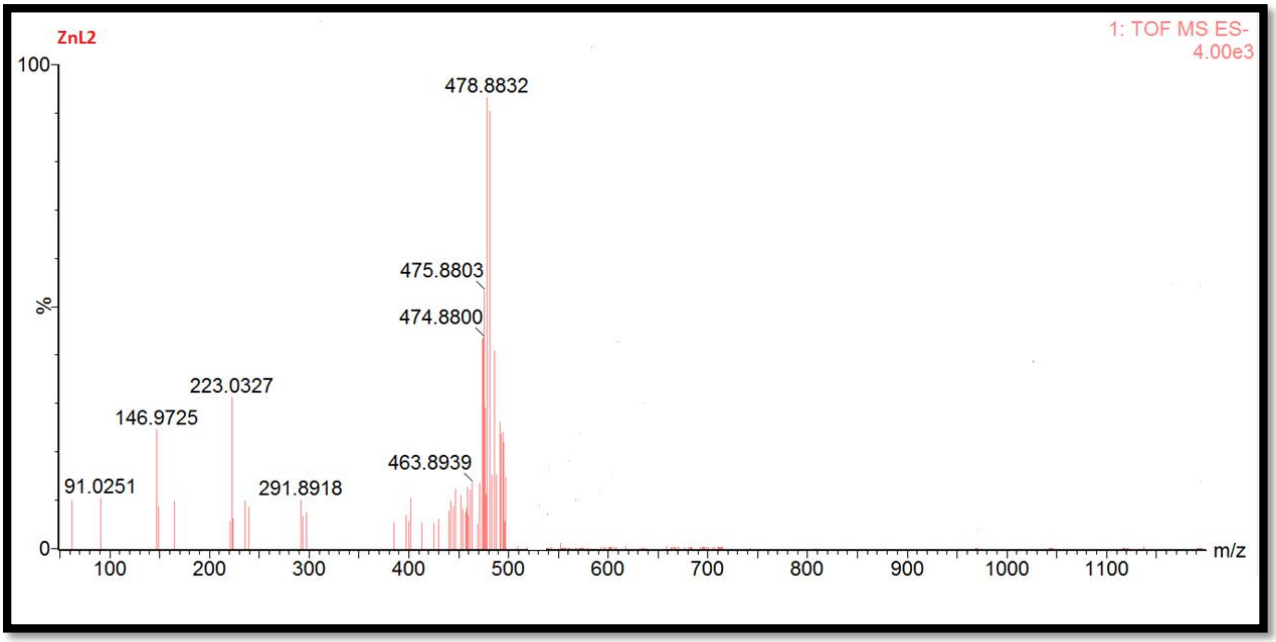

Figure 18: Mass spectrum of [ZnL2(H_2O)] complex

SEM-EDX analysis

To evaluate the surface morphology of the ligands and their complexes, scanning electron microscopy (SEM) was used. Slim rod-shaped and feather-like shaped nanostructures were observed for HL1 and HL2 respectively. While, a block-shaped composed of nano-sheets is grown in the complexes but differs in shapes and sizes which could be due to the differences in

halo-substituents on the ligands (Figure 19). The morphological changes in the complexes compared with the ligands further confirmed the formation of the complexes. Furthermore, the ligands and their complexes were analysed using EDX. The ligands show presence of C, N, O, Cl and Br. However, the complexes displayed presence of Zn in addition to elemental contents of the ligands, indicating the formation of the complexes (Figure 20).

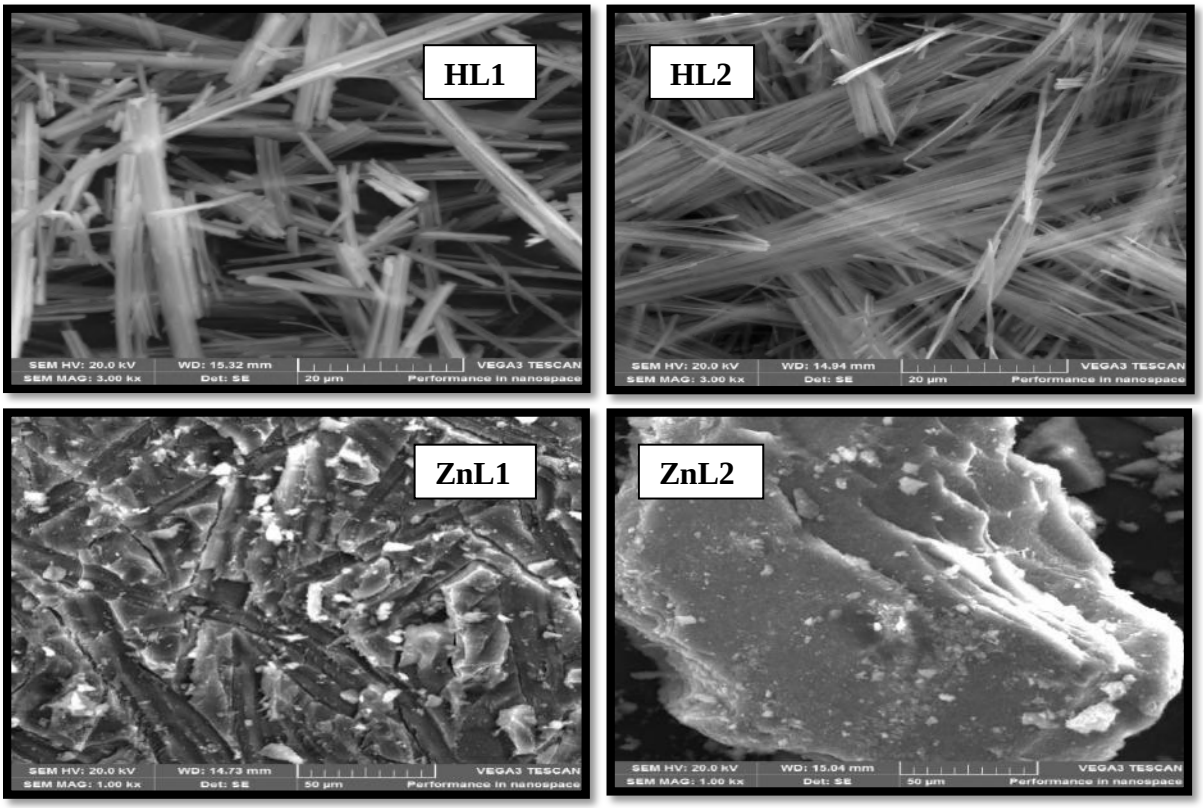

Figure 19: SEM images of ligands and their complexes

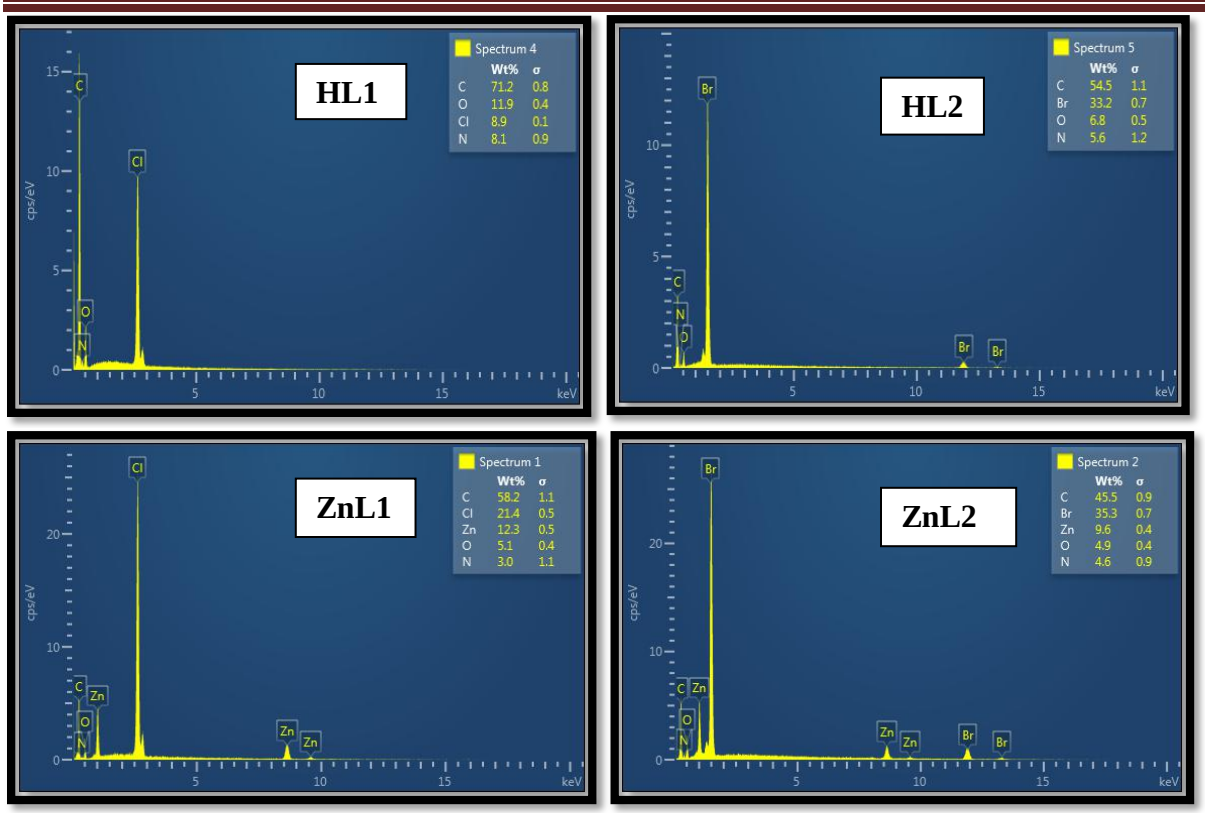

Figure 20: EDX micrograph of ligands and their complexes

Antimicrobial study

Schiff bases and their metal complexes are known to have potent antimicrobial activities against different multidrug-resistant strains [64, 65]. Herein, the free ligands and their metal complexes were screened against Gram-positive strains (*S. aureus* ATCC-25923 and *B. subtilis* ATCC-6633) and Gram-negative strains (*E. coli* ATCC-25922 and *K. pneumoniae* ATCC-13883) using *in vitro* disc diffusion method, with concentration of 5 and 10 mg/mL of the compounds. Dimethyl sulfoxide (DMSO) and ciprofloxacin were utilized as negative and positive controls, respectively. The results obtained were recorded in Table 4 and Figure 21. In general, both the ligands and their complexes were less active against the tested organism compared to the standard drug. However, it can be seen that the free ligands exhibited less antimicrobial activity on all the pathogens, compared to their metal complexes with [ZnL1(H_2O)] showing enhanced activity on Gram-negative than Gram-positive and [ZnL2(H_2O)] showed better activity on Gram-positive than Gram-negative. Similar trend was observed on the ligands. The activity demonstrated by the ligands is due to the formation of hydrogen bonding between the phenolic protons with the active center of the bacterial cell wall. The hydrogen bond tend to disrupt the

cellular activity of bacteria [66]. The increase in the antimicrobial activity of complexes can be explained on the basis of principle of chelation theory. Chelation theory stated that when ligands coordinate metal ions, it resulted to decrease in the polarity of the metal ion and thereby result to the overlapping between the orbital of the ligand with that of the metal ion for eased of interference with cellular activity [66]. It is also worthy to mention that the halo-substituent on the ligands did not causes significant changes on the antimicrobial activity of the complexes.

The MIC data of the compounds is presented in Table 5. From the result, it can be seen that the free ligands and their complexes showed MIC result higher than the control drug. The ligands presented lowest MIC of 16 µg/mL on either Gram-positive or Gram-negative respectively. However, the complexes showed lowest MIC of 4 µg/mL on the same organisms.

Table 4: The results of the antimicrobial studies of the ligands and their complexes[a]

Compound	**Conc. (mg/mL)**	**Zone of inhibitions (mm)**			
		S. aureus	***B. subtilis***	***E.coli***	***K. Pneumonioe***
HL1	5	12±1.0	8.5±0.5	13±1.0	12.5±0.6
	10	23±1.0	15.7±1.2	26.3±1.5	25±2.0
HL2	5	13.5±0.5	12 ±0.3	10.3±1.0	7±0.5
	10	23.7±1.5	23±0.8	19.7±2.1	13±2.5
[ZnL1(H_2O)]	5	20±0.6	14±0.6	24±0.6	22±0.6
	10	38.8±0.8	27.3±1.5	45±1.0	43±1.5
[ZnL2(H_2O)]	5	21±0.6	19±0.6	17±0.6	11.7±0.6
	10	40±1.0	36±1.5	34±2.0	23±1.0
Cipro[c]	5	22.5±0.5	24±0.3	26±0.3	23±0.8
	10	42.5±0.5	45±1.5	47±1.0	45±0.8
DMSO[b]	-	NA	NA	NA	NA

NA = no activity, the values presented are the mean of the three closely related experimental values.
[b]DMSO is included as a negative control based on its usage as solvent carrier for the test compounds.

Table 5: Minimum inhibitory concentration (MIC) data of the ligands and their complexes

Compound	**MIC (µg/mL)**			
	Sa	**Bs**	**Ea**	**Kb**
HL1	32	32	16	16
HL2	16	16	32	32
[ZnL1(H_2O)]	4	4	8	8
[ZnL2(H_2O)]	8	8	4	4
Cipro	2	0.25	0.25	0.25

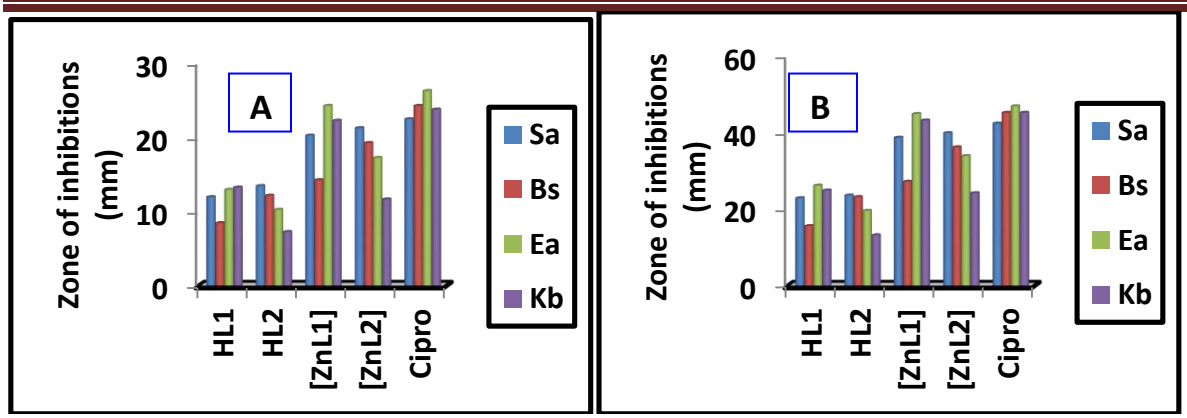

Figure 21: Antimicrobial activity of the ligands and their complexes (**A**) at conc. of 5 mg/mL, and (**B**) at conc. 10 mg/mL.Sa = *Staphylococcus aureus*, Bs = *Bacillus subtilis*, Ea = *Escherichia coli*, Kb = *Klebsiella pneumoniae* and Cipro = Ciprofloxacin

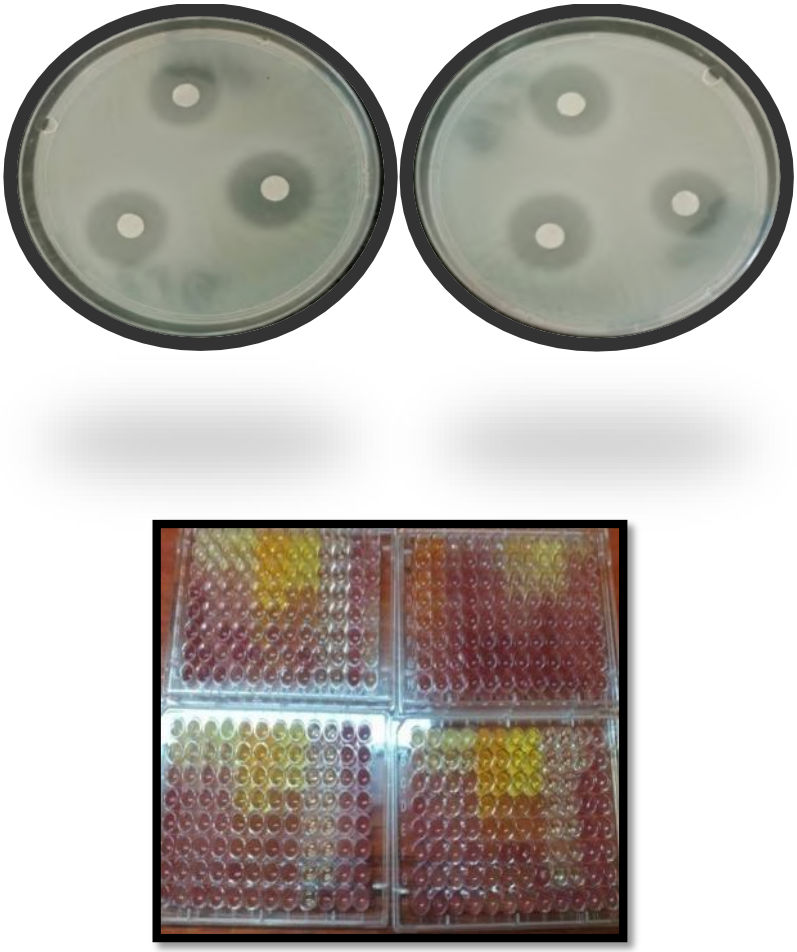

Figure 22: Representative culture and 96 well plates for the antimicrobial study

Antioxidant activity studies

DPPH Free-radical scavenging activity

Accumulation of free radical in the body is responsible for many diseases in human. Antioxidant compounds help in mopping up free radicals and reduce their effect in the body [67]. Schiff bases or their metal complexes are known to scavenged free radicals [68]. To evaluate the antioxidant potentials of the synthesised Schiff bases and their complexes, DPPH radical scavenging assay was used. DPPH produces violet or purple color in methanolic solution, and changes to yellow in the presence of antioxidants. The results of DPPH radical scavenging ability of the ligands and their complexes compared with positive control (ascorbic acid) are presented in Table 6 and Figure 23A. The result showed that the scavenging activity of the compounds increases as the concentration increased from 10 to 150 $\mu g.mL^{-1}$. The DPPH radical scavenging rate of the complexes is higher than that of the free ligands, and it is positively correlated with the concentration. It can also be seen that HL2 and [ZnL2(H_2O)] showed higher DPPH scavenging ability compared with HL1 and [ZnL1(H_2O)] respectively. However, the positive control displayed DPPH scavenging ability higher than the complexes with IC_{50} 3.0 µg/mL. At concentration of 20 µg/mL, the DPPH radical scavenging rate of the complexes [ZnL1(H_2O)] and [ZnL2(H_2O)] reached 50 and 55 µg/mL and those of the ligands HL1 and HL2 were 43 and 45 µg/mL respectively. Also, [ZnL1(H_2O)] and [ZnL2(H_2O)] showed IC_{50} 19 and 5.7 $\mu g.mL^{-1}$. HL1 and HL2 displayed IC_{50} 55.7 and 42.9 $\mu g.mL^{-1}$ respectively. This result showed that complexes have stronger DPPH radical scavenging ability compared to the ligands. Sparingly, bromo substituted ligand (HL2) and its complex showed higher scavenging activity than the chloro substituted. The higher reactivity properties of chlorine atom is expected to improve the activity than the bromo atom, but the size of bromine atom might have resulted to more stability of the compound and thereby promote better activity compared to the chloro substituted counterpart [69].

Table 6: DPPH radical scavenging activity data of the ligands and their complexes

Compound	**Concentrations ($\mu g.mL^{-1}$)**					
	10	**20**	**50**	**100**	**150**	**IC_{50}**
HL1	35.2±0.3	43.0±0.6	56.3.0±1.0	62.0±1.0	64.0±1.0	55.7
HL2	38.3±0.6	45.3±0.6	58.1±1.0	64.0±1.0	67.0±0.0	42.9
[ZnL1(H_2O)]	43.0±1.0	50.5±0.5	64.7±0.6	72.7±0.6	84.1±1.0	19.0
[ZnL2(H_2O)]	46.7±0.6	54.2±0.6	68.0±1.0	76.0±1.0	88.0±1.0	5.7
ASA	47.3±0.3	55.0±1.2	70.0±1.5	78.0±0.3	89.7±1.1	3.0

Anova: p-value = 0.000; p-value < 0.05 at n = 3, compared to standard ascorbic acid was considered statistically significant (By One-way ANOVA, Turkey HSD). **ASA** = Ascorbic acid

ABTS˙ radical scavenging activity

ABTS˙ radical scavenging ability of the ligands, their complexes and ascorbic acid (positive control) were evaluated using concentration of 5, 10, 15, 20 and 40 µg/mL. The results obtained are presented in Table 7 and Figure 23B. The ligands and their complexes showed dose-dependent scavenging ability. In general, the complexes showed about 10% more radical scavenging ability than the ligands and about 3% less than the positive control. Similarly, HL2 and [ZnL2(H_2O)] demonstrated higher ABTS˙ radical scavenging ability than HL1 and [ZnL1(H_2O)]. The IC_{50} of HL1 and HL2 were found to 27.7 and 23.0 µg.mL^{-1}. The complexes, [ZnL1(H_2O)] and [ZnL2(H_2O)] showed $IC_{50}$of 19.3 and 15.3 µg.mL^{-1} respectively, while, the positive control gave IC_{50} of 13.3 µg/mL. The bromo substituted ligand and its complex showed similar trend as in the case of DPPH radical scavenging activity.

Table 7: ABTS˙ radical scavenging activity data of the ligands and their complexes

Compound	**Concentrations (µg.mL^{-1})**					
	5	**10**	**20**	**30**	**40**	**IC_{50}**
HL1	28.1±1.0	36.1±1.0	43.1±1.0	51.3±1.2	61.0±1.0	27.7
HL2	32.0±0.0	41.3±1.5	47.0±1.0	56.0±1.0	65.0±2.0	23.0
[ZnL1(H_2O)]	34.3±0.6	43.0±2.0	50.0±0.6	58.0±2.0	75.0±1.0	19.3
[ZnL2(H_2O)]	38.0±1.0	47.2±0.3	54.0±1.0	63.2±0.3	78.0±0.0	15.3
ASA	40.0±0.3	49.3±1.1	56.2±0.9	66.1±0.7	80.1±1.3	13.2

Hydroxyl radical (˙OH) scavenging activity

Hydroxyl radicals have active chemical properties, react faster and cause more harm to the body than other free radicals. Within a biological system, hydroxyl radicals invade the cell membrane, disrupt genetic materials and subsequently leading to cell death/mutation [70]. Hence, scavenging hydroxyl radicals by testing the complexes is aimed at evaluating the ability of the compounds to mop up the free radical. The synthesised ligands and their Zn(II) complexes demonstrated the ability to scavenge the hydroxyl free radicals and reached maximum scavenging rate at concentration of 20 µg.mL^{-1} (Table 8 and Figure 23C). At lower concentration, the hydroxyl radical scavenging of the ligands was found to be higher than that of the complexes but 2-3% lower than the positive control ($p< 0.05$) and this could be due to the influence of active phenolic functional group of the ligands. However, as the concentration

increased from 15 to 20 μg.mL^{-1}, the scavenging rate of the complexes on hydroxyl free radicals was observed to be higher than the ligands ($p<0.05$). This increase could be explained based on the principle of chelation theory [71]. Therefore, it could be concluded that within a particular concentration range, the scavenging ability of the complexes is more than the ligands but less than the positive control ($p < 0.05$).

Table 8: Hydroxyl radical ($^{\bullet}$OH) scavenging activity data of the ligands and their complexes

Compound	**Concentrations (μg.mL^{-1})**					
	5	**10**	**15**	**20**	**25**	**IC$_{50}$**
HL1	30.0 ± 1.0	37.0±1.7	53.0±0.5	58.0±2.0	50.0±0.5	18.6
HL2	33.0±3.0	42.0±2.6	55.0±0.5	62.0±2.6	53.0±0.5	15.8
[ZnL1(H$_2$O)]	25.0±1.0	35.0±0.5	68.0±1.0	73.0±0.9	60.0±0.5	14.0
[ZnL2(H$_2$O)]	28.0±2.0	38.0±0.0	70.0±0.2	76.0±0.5	64.0±0.5	12.6
ASA	35.0±1.5	45.0±0.8	76.0±0.2	79.0±0.3	82.0±2.6	9.8

Superoxide radical ($O_2^{-\bullet}$) scavenging activity

The ligands and their complexes were evaluated for their scavenging ability on superoxide free radical and compared with positive control (ascorbic acid). The results obtained are shown in Table 9 and Figure 23D. The ligands and their complexes displayed scavenging ability on superoxide radicals in a concentration dependent manner. The complexes showed scavenging rate 9% more than the ligands at all concentrations. Similarly, [ZnL2(H$_2$O)] is more active than [ZnL1(H$_2$O)]. Similarly, HL1 is less active than HL2. The higher superoxide radical scavenging activity of Hl2 and [ZnL2(H$_2$O)] than HL1 and [ZnL1(H$_2$O)] could be attributed to bromide substituent on HL2 moiety. However, both [ZnL2(H$_2$O)] and [ZnL1(H$_2$O)] showed radical scavenging activity less than the positive control. The IC$_{50}$ of the ligands and their complexes were found to be 42.8 and 38.5 μg/mL, and 32.4 and 27.0 μg/mL respectively. The positive control showed IC$_{50}$of 19.4 μg.mL^{-1}. Therefore, it can be concluded that the complexes exhibited remarkable superoxide radical scavenging ability at ($p < 0.05$).

Table 9: Superoxide radical ($O_2^{-\bullet}$) scavenging activity data of the ligands and their complexes

Compound	**Concentrations (μg.mL^{-1})**					
	5	**10**	**15**	**20**	**40**	**IC$_{50}$**
HL1	15.0±0.7	27.0±0.5	35.0±0.0	39.0±04	44.0±1.0	42.8
HL2	18.0±0.5	33.0±0.3	38.0±1.0	43.0±0.5	47.0±0.0	38.5
[ZnL1(H$_2$O)]	22.0±0.8	35.0±0.4	41.0±1.0	46.0±0.5	52.0±1.0	32.4
[ZnL2(H$_2$O)]	25.0±0.7	38.0±0.9	45.0±1.0	51.0±0.9	56.0±1.0	27.0
ASA	29.0±0.5	41.0±1.0	48.0±1.0	57.0±0.5	68.0±1.0	19.4

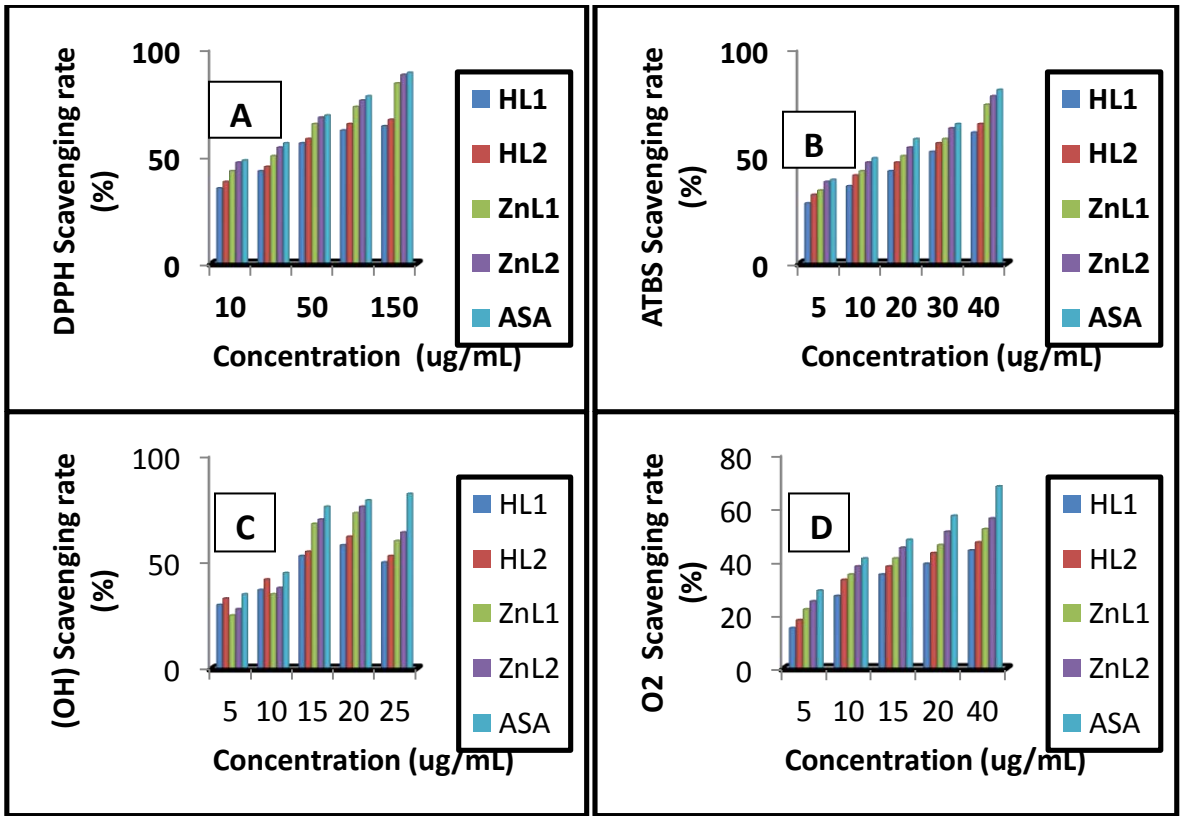

*Figure 23: Antioxidant activity. Scavenging ability of the ligands and their complexes on (A) DPPH free radicals, (**B**) ABTS* free radicals, (**C**) *OH free radical, and (**D**) O_2^{*-} superoxide free radicals*

CONCLUSION

Two Zn(II) metal complexes were synthesised from two *ONO* donor ligands. The ligands and their complexes were characterized using various characterization techniques. From these characterization techniques, the formation of the ligands and their complexes was confirmed. *In vitro* antimicrobial screening of the ligands and their complexes against Gram-positive and Gram-negative bacteria revealed that the metal complexes have better activity than their free ligands. The [ZnL1(H_2O)] showed enhanced activity against Gram-negative, and [ZnL2(H_2O)]

was found to be more active against Gram-positive bacteria. In general, both complexes have lower MIC value of 4 μg/mL and higher MIC of 8 μg/mL respectively and [ZnL2(H_2O)] exhibiting medium to higher activity across the organism. In addition, the ligands and their complexes were evaluated for antioxidant activities using (DPPH radicals scavenging, ATBS$^{\bullet}$ radicals scavenging, hydroxyl radicals scavenging and superoxide radicals scavenging). The results revealed varying degree of radical scavenging activities, with the complexes showing higher scavenging rate than the free ligands. These results provide a strong platform for a medicinal chemistry approach to fine tune the characteristic and activity of the compounds.

REFERENCES

[1] Bhaskar, R.S., Ladole, C.A., Salunkhe, N.G., Barabde, J.M. & Aswar, A.S.(2020). Synthesis, characterization and antimicrobial studies of novel ONO donor hydrazone schiff base complexes with some divalent metal (II) ions.*Arabian Journal of Chemistry*. 13(8),6559-6567.

[2].Al-Rasheed, H.H., Sholkamy, E.N., Al-Alshaik, M., Siddiqui, M.R.H., Al-Obaidi, A.S. & El-Faham, A. (2018). Synthesis, characterization, and antimicrobial studies of novel series of 2, 4-Bis (hydrazino)-6-substituted-1, 3, 5-triazine and their schiff base derivatives. *Journal of Chemistry*.1, 1-13.

[3]. Raczuk, E., Dmochowska, B., Samaszko-Fiertek, J. & Madaj, J. (2022). Different schiff bases—structure, importance and classification. *Molecules*. 27(3), 787-900.

[4]. Alorini, T.A., Al-Hakimi, H.N., Saeed, S.E., Alhamzi, E.H.L. & Albadri, AE. (2022). Synthesis, characterization, and anticancer activity of some metal complexes with a new schiff base ligand.*Arabian Journal of Chemistry*. 15(2), 103559-103577.

[5]. Saritha, T. & Metilda, P. (2021). Synthesis, spectroscopic characterization and biological applications of some novel Schiff base transition metal (II) complexes derived from curcumin moiety. *Journal of Saudi Chemical Society*. 25(6), 101245-101259.

[6]. Ayyavoo, T., Kesavan, M.P., Kumar, S.M., Ravi, L., Bhaskar, R., Rajagopal, G. & Rajesh, J. (2021). Synthesis, structure, DNA/protein molecular docking and biological studies of hydrazone ligand derived Cu (II) and VO (IV) complexes.*Inorganica Chimica Acta*. 526, 120543-120560.

[7]. Cui, Y.M., Qiao, L., Li, Y., Wang, Q., Chen, W. & Yan, W.X. (2017). Synthesis, crystal structures and catalytic epoxidation properties of dioxomolybdenum (VI) complexes with

hydrazone ligands.*Transition Metal Chemistry*. 42(1), 51-56.

[8]. Devi, J. & Pachwania, S. (2021) Synthesis, characterization, in vitro antioxidant and antimicrobial activities of diorganotin (IV) complexes derived from hydrazide Schiff base ligands. *Phosphorus, Sulfur, and Silicon and the Related Elements*. 196(12), 1049-1060.

[9]. Omidi, S. & Kakanejadifard, A. (2020). A review on biological activities of Schiff base, hydrazone, and oxime derivatives of curcumin.*RSC Advances*. 10(50), 30186-30202.

[10]. Khan, T., Zehra, S.A.A., Fatima, U. & Lawrence, A.J. (2015). Medicinal utility of some Schiff bases and their complexes with first transition series metals*:* A-Review. *New Journal of Chemistry*. 29(3), 45-73.

[11]. Lv, Y., Meng, J., Li, C., Wang, X., Ye, Y. & Sun, K. (2021).Update on the synthesis of *N*-Heterocycles via cyclization of hydrazones (2017–2021). *Advanced Synthesis and Catalysis*. 363(23), 5235-5265.

[12]. Abdel-Aziz, A.A.M., El-Azab, A.S., Al-Saif, N.A., Obaidullah, A.J., Al-Obaid, A.M. & Al-Suwaidan, I.A. (2021). Synthesis, potential antitumor activity, cell cycle analysis, and multitarget mechanisms of novel hydrazones incorporating a 4-methylsulfonylbenzene scaffold: a molecular docking study.*Journal of Enzyme Inhibition and Medicinal Chemistry*. 36(1), 1520-1538.

[13]. Ragab, A., Elsisi, D.M., Ali, O.A.A., Abusaif, M.S., Askar, A.A., farag, A.A. & Ammar, Y.A. (2022). Design, synthesis of new novel quinoxalin-2 (1H)-one derivatives incorporating hydrazone, hydrazine, and pyrazole moieties as antimicrobial potential with in-silico ADME and molecular docking simulation.*Arabian Journal of Chemistry*.. 15(1), 103497-103516.

[14]. Suryawanshi, N.J., Pethe, G.B., Yaul, A.R. & Aswar, A.S. (2014). Synthesis, characterization and biological studies of some transition metal chelates derived from hydrazone Schiff base ligand. *Jordan Journal of Chemistry*. 9(3), 199-216.

[15]. Dongare, G. & Aswar, A. (2021). Synthesis, spectral characterization, thermo-kinetic and biological studies of some complexes derived from tridentate hydrazone Schiff base. *Journal of Saudi Chemical Society*. 25(10), 101325-101338.

[16]. Al-Qadsy, I., Al-Odayni, A.B., Saeed, W.S., Alrabie, A., Al-Adhreai, A., Al-Faqeeh, L.A.S., Alghamdi, P.L.A. & Farooqui, M. (2021). Synthesis, characterization, single-crystal x-ray structure and biological activities of [(Z)-N′-(4-Methoxybenzylidene) benzohydrazide–Nickel (II)] Complex.*Crystals*. 11(2), 110-118.

[17]. Faiq, B. & Ahmad, B.O. (2021). Synthesis and characterization of some divalent transition metal complexes with acid hydrazone ligand. *Zanco Journal of Pure and Applied Sciences*. 33(5), 85-94.

[18]. Daravath, S., Narendrula, V.K. & Marri, P.K. (2021). Synthesis, characterization, docking and antimicrobial activity studies of binuclear Co (II) and Ni (II) complexes of bis aroylhydrazone and phenanthroline. *Bulletin of the Chemical Society of Ethiopia*. 35(3), 499-511.

[19]. Ridhorkar, B., D., Ramteke, A.A., Vyawahare, Y.K. & Yaul, A.R. (2021). Synthesis, characterization and biological screening of Ti (III), Cr (III), Fe (III) and UO2 (VI) mononuclear complexes of hydrazone Schiff base ligand containing NON moiety. *AIP Conference Proceedings*. 2369(1), 020029-020043.

[20]. Aliyu, H. & Adamu, H. (2021). Synthesis, characterization and antimicrobial activities of Ni(II) and Cu(II) complexes with schiff base derived from 2-acetyl-5-methylfuran glyoxime hydrazone. *FUDMA Journal of Sciences*. 5(4), 268-274.

[21]. Tolan, D.A., Kashar, T.I., Yoshizawa, K. & El-Nahas, A.M. (2021). Synthesis, spectral characterization, density functional theory studies, and biological screening of some transition metal complexes of a novel hydrazide–hydrazone ligand of isonicotinic acid. *Applied Organometallic Chemistry*. 35(6), e6205-62029.

[22]. Aly, S. & Fathalla, S. (2020). Preparation, characterization of some transition metal complexes of hydrazone derivatives and their antibacterial and antioxidant activities. *Arabian Journal of Chemistry*. 13(2), 3735-3750.

[23]. Philip, J.E., Antony, S.A., Eeettiniikunnathil, S.J., Kunip, M.P. & Velayudhan, M.P. (2018). Design, synthesis, antimicrobial and antioxidant activity of 3-formyl chromone hydrazone and their metal (II) complexes. *Inorganica Chimica Acta*. 469, 87-97.

[24]. Hussain, I., Ullah, A., Khan, A.U., Khan, W.U. & Ullah, R. (2019). Synthesis, characterization and biological activities of hydrazone Schiff base and its novel metals complexes. *Sains Malaysiana*. 48(7), 1439-1446.

[25]. Mandlik, P.R. & Deshmukh, P.K. (2020). Synthesis, spectroscopic characterization, thermal analysis and biological studies of hydrazone Schiff base and its Co (II), Cu (II), Th (IV) and Zr (IV) metals complexes.*Saudi Journal of Medicinal Pharmaceutical Science*. 6(12), 724-732.

[26]. Bhovi, V.K., Bharathi, K., Melinmath, S.P., Basavanna, V. & Ningaiah, S. (2021).

Transition metal (II) complexes of (E)-N-(4-methylbenzylidene)-2-((Z)-(4-methylbenzylidene) amino) benzamides: Synthesis, characterization and their biological evaluation. *Inorganic Chimica Acta*. 603, 33-48.

[27]. Mohamed, A. (2017). Structure studies of the prepared novel hydrazone Schiff's base complexes using spectroscopic, thermal analyses and their biological activities. *Journal of Transition Metal Complexes*. 1, 1-10.

[28]. Moradinia, E., Mansounia, M., Aramesh-Boroujeni, Z. & Bordbar, A.K. (2019). New transition metal complexes of 9, 10-phenanthrenequinone p-toluyl hydrazone Schiff base: Synthesis, spectroscopy, DNA and HSA interactions, antimicrobial, DFT and docking studies. *Applied Organometallic Chemistry*. 33(5), e4893-48516.

[29]. Abera, S., Dessalegn, T. & Endale, M. (2018). Synthesis and antibacterial activity of phenylhydrazone Schiff base derivatives and their copper (II) complexes. *Synthesis*, 10(6s), 57-68.

[30]. Bonnett, S.A., Dannison, D., Files, M., Bajpai, A. & Parish, T. (2018). A class of hydrazones are active against non-replicating Mycobacterium tuberculosis. *PLoS One*. 13(10), e0198059.

[31]. Mandewale, M.C., Thorat, B., Shelke, D. & Yamgar, R. (2015). Synthesis and biological evaluation of new hydrazone derivatives of quinoline and their Cu (II) and Zn (II) complexes against Mycobacterium tuberculosis. *Bioinorganic Chemistry and Applications*. 6(2), 1098-10108.

[32]. de Faria, C.F., Moreira, T., Lopes, P., Costa, H., Krewell, J.R., Barton, C.M., Santos, S., Goodwin, D., Machado, D., Viveiros, M. & Machuqueiro, M. (2021). Designing new antitubercular isoniazid derivatives with improved reactivity and membrane trafficking abilities. *Biomedicine and Pharmacotherapy*. 144, 112362-112376.

[33]. Prabhakara, C.T., Patil, S.A., Toragalmath, S.S., Kinnal, S.M. & Badami, P.S. (2016). Synthesis, characterization and biological approach of metal chelates of some first row transition metal ions with halogenated bidentate coumarin Schiff bases containing N and O donor atoms. *Journal of Photochemistry and Photobiology B: Biology*. 157, 1-14.

[34]. Hejchman, E., Kruszewska, H., Maciejewska, D., Sowirka-Taciak, B., Tomczyk, M., Sztokfisz-ignasiak, A., Jankowski, J. & Izabela, M.B. (2019). Design, synthesis, and biological activity of Schiff bases bearing salicyl and 7-hydroxycoumarinyl moieties.*Monatshefte für Chemie-Chemical Monthly*. 150(2), 255-266.

[35]. Krężel, A. & Maret, W. (2016). The biological inorganic chemistry of zinc ions.*Archives of Biochemistry and Biophysics*. 611, 3-19.

[36]. Hudson, D.L., Layton, A.N., Field, T.R., Bowen, A.J., Wolf-watz, H., Elofsson, M., Stevens, M.P. & Galyov, E.E. (2007). Inhibition of type III secretion in Salmonella enterica serovar Typhimurium by small-molecule inhibitors. *Antimicrobial Agents and Chemotherap*.,51(7), 2631-2635.

[37]. Tree, J.J., Wang, D., Mclnally, C., Mahajan, A., Layton, A., Houghton, I., Elofsson, M., Stevens, M.P., Gally, D.L. & Roe, A.J. (2009). Characterization of the effects of salicylidene acylhydrazide compounds on type III secretion in Escherichia coli O157: H7. *Infection and Immunity*.**77**(10), 4209-4220.

[38]. Layton, A.N., Hudson, D.L., Thompson, A., Hinton, J.C., Stevens, J.M., Galyov, E.E. & Stevens M.P. (2010). Salicylidene acylhydrazide-mediated inhibition of type III secretion system-1 in Salmonella enterica serovar Typhimurium is associated with iron restriction and can be reversed by free iron.*FEMS Microbiology Letters*. 302(2), 114-122.

[39]. Ainscough, E.W., Brodie, A.M., Denny, W.A., Finlay, G.J., Gothe, S.A. & Ranford, J.D. (1999). Cytotoxicity of salicylaldehyde benzoylhydrazone analogs and their transition metal complexes: quantitative structure–activity relationships.*Journal of Inorganic Biochemistry*. **77**(3-4), 125-133.

[40]. Mohan, B., Choudhary, M., Bhanti, S., Jana, A., Das, N., Mohammed, S., Al-Sehem, A.G. & Kumar, S. (2019). Syntheses, characterizations, crystal structures and efficient NLO applications of new organic compounds bearing 2-methoxy-4-nitrobenzeneamine moiety and copper (II) complex of (E)-N'-(3, 5-dichloro-2-hydroxybenzylidene) benzohydrazide.*Journal of Molecular Structure*. 1190, 54-67.

[41].Toh-Boyo, G.M., Njongi, R.N., Babatte, E.M. & Nfor, E.N. (2021). Synthesis, spectroscopic, molecular modeling and anti-fungal studies of some divalent metal complexes of 4-Hydroxyacetophenone Isonicotinoyl Hydrazone. *Open Journal of Inorganic Chemistry*. 11(3), 95-109.

[42]. Renjitha, J. & Thara, G. (2017). Synthesis and spectral studies of zinc (II) complexes of a Schiff base derived from isatin hydrazone and 2-hydroxy naphthaldehyde.*AIP Conference Proceedings*. 5(3), 68-76.

[43]. More, M., Joshi, P.G., Mishira, Y.K. & Khanna, P.K. (2019). Metal complexes driven from Schiff bases and semicarbazones for biomedical and allied applications: a review. *Materials*

Today Chemistry. 14, 100195.

[44]. Naureen, B., Miana, G.A., Shahid, K., Asghar, M., Tanveer, S. & Sanwar, A. (2021). Iron (III) and zinc (II) monodentate Schiff base metal complexes: Synthesis, characterisation and biological activities.*Journal of Molecular Structure*. 123, 129946.

[45]. Abdel-Rahman, L.H., Ismail, N.M., Ismael, M., Abu-Dief, A.M. & Ahmed, E.A.H. (2017). Synthesis, characterization, DFT calculations and biological studies of Mn (II), Fe (II), Co (II) and Cd (II) complexes based on a tetradentate ONNO donor Schiff base ligand.*Journal of Molecular Structure*. 1134, 851-862.

[46]. Hashem, H.E., Mohammed, E.A., Farag, A.A., Negm, N.A. & Azmy, E.A. (2021). New heterocyclic Schiff base-metal complex: Synthesis, characterization, density functional theory study, and antimicrobial evaluation. *Applied Organometallic Chemistry*. 35(9), e6322-6336.

[47]. Tyagi, P., Chandra, S., Saraswat, B.S. & Yadav, D. (2015). Design, spectral characterization, thermal, DFT studies and anticancer cell line activities of Co (II), Ni (II) and Cu (II) complexes of Schiff bases derived from 4-amino-5-(pyridin-4-yl)-4H-1, 2, 4-triazole-3-thiol. *Spectrochimica Acta Part A: Molecular and Biomolecular Spectroscopy*. 145, 155-164.

[48]. Othman, I.M., Gad-Elkareem, M.A., El-Naggar, M., Nossier, E.S. & Amr, A.E.G.E. (2019). Novel phthalimide based analogues: Design, synthesis, biological evaluation, and molecular docking studies. *Journal of Enzyme Inhibition and Medicinal Chemistry*. 34(1), 1259-1270.

[49]. Sobola, A.O., Watkins, G.M., Shaibu, R.O., Adewuyi, S. & Amolegbe, S.A. (2021). Synthesis, characterization and antimicrobial activity of copper (II) Schiff base adducts of some p-substituted aniline Schiff bases. *Bulletin of the Chemical Society of Ethiopia*. 35(1), 33-42.

[50]. Pagning, A.L.N., Lateef, M., Tapondjou, L.A., Kuiate, J.R., Ngnokam, D. & Ali, M.S. (2016). New triterpene and new flavone glucoside from Rhynchospora corymbosa (Cyperaceae) with their antimicrobial, tyrosinase and butyrylcholinesterase inhibitory activities. *Phytochemistry Letters*. 16, 121-128.

[51]. Turecka, K., Chylewska, A., Rychlowski, M., Zakrzewska, J. & Waleron, K. (2021). Antibacterial activity of Co (III) complexes with diamine chelate ligands against a broad spectrum of bacteria with a DNA interaction mechanism. *Pharmaceutics*. 13(7), 946-957.

[52]. Nyawade, E.A., Onani, M.O., Meyers, S. & Dube, P. (2021). Synthesis, characterization and antibacterial activity studies of new 2-pyrral-L-amino acid Schiff base palladium (II) complexes. *Chemical Papers*. 74(11), 3705-3715.

[53]. Karrouchi, K., Fettach, S., Radi, S., Taoufik, J. Mabkhot, Y.N., Alterary, S., Faouzi, M.E. & Ansar, M. (2019). Synthesis, characterization, free-radical scavenging capacity and antioxidant activity of novel series of hydrazone, 1, 3, 4-oxadiazole and 1, 2, 4-triazole derived from 3, 5-dimethyl-1H-pyrazole. *Letters in Drug Design & Discovery*. 16(7), 712-720.

[54]. Onwudiwe, D.C. & Ekennia, A.C. (2017). Synthesis, characterization, thermal, antimicrobial and antioxidant studies of some transition metal dithiocarbamates. *Research on Chemical Intermediates*. 43(3), 1465-1485.

[55]. Wang, X., He, S., Yuan, L., Deng, H. & Zheng, Z. (2021). Synthesis, structure characterization, and antioxidant and antibacterial activitys study of iso-orientin–Zinc complex. *Journal of Agricultural and Food Chemistry*. 69(13), 3952-3964.

[56]. Aldeen, M.G.N., Mansour, R. & AlJoubbeh, M. (201). The effect of food additives and cooking on the antioxidant properties of purslane. *Nutrition and Food Science*. 12(2), 1-13.

[57]. Ganji, S.M., Singh, H.& Friedman, M. (2019). Phenolic content and antioxidant activity of extracts of 12 melon (Cucumis melo) peel powders prepared from commercial melons.*Journal of Food Science*. 84(7), 1943-1948.

[58]. Refat, M.S., Gaber, A., Alsanie, W.F., Kobeasy, M.I., Zakaria, R. & Alam, K. (2021). Utilization and simulation of innovative new binuclear Co (II), Ni (II), Cu (II), and Zn (II) diimines schiff base complexes in sterilization and coronavirus resistance (Covid-19).*Open Chemistry*. 19(1), 772-784.

[59]. Ashrafuzzaman, M. D., Camelia, F.K., Mahmud, A.A., Pramanik, M.D., Nahar, K. & Haque, M. (2021). Bioactive mixed ligand metal complexes of Cu (II), Ni (II), And Zn (II) ions: synthesis, characterization, antimicrobial and antioxidant properties. *Journal of the Chilean Chemical Society*. 66(3), 5295-5299.

[60]. Savcı, A., Buldurun, K. & Kırkpantur, G. (2021). A new Schiff base containing 5-FU and its metal complexes: synthesis, characterization, and biological activities. *Inorganic Chemistry Communications*. 134, 109060.

[61]. Shekhawat, A., Singh, N. & Chundawat, N. (2022). Synthesis, characterization and biological activities of schiff's base metal complexes derived from hydroxy trizene and

aromatic aldehyde. *Journal of Scientific Research*. 14(1), 387-394.

[62]. Abbas, H.H. (2016). Synthesis, characterization, kinetic and thermodynamic parameters evaluation from TG-DTA analysis of Cu (II), Co (II) and Mn (II) complexes with two phenol Schiff bases.*European Journal of Chemistry*. 7(4), 436-441.

[63]. Cui, Y., Liu, J., Lin, J., Liu, J. & Chen, W. (2016). Synthesis, characterization and x-ray crystal structures of cis-dioxomolybdenum (VI) complexes of similar tridentate aroylhydrazone Schiff bases with catalytic epoxidation activity. *Acta Chimica Slovenica*. 63(2), 279-286.

[64]. Malik, M.A., Dar, O.A., Gull, P., Wani, M.Y. & Hashmi, A.A. (2018). Heterocyclic Schiff base transition metal complexes in antimicrobial and anticancer chemotherapy.*Medicinal Chemistry Communication*. 9(3), 409-436.

[65]. Ceramella, J., Lacopetta, D., Catalana, A., Crilla, F., Lappano, R. & Sinicropi, M.S. (2022). A review on the antimicrobial activity of schiff bases: Data collection and recent studies. *Antibiotics*. 11(2), 191-204.

[66]. Waziri I., Fugu, M.B., Zarma H.A., Isa B., & Askira, N.K. (2022). Transition metal complexes derived from 1*H*-Imidazole ligand: synthesis, characterization, cyclic voltammetric studies and *in vitro* antibacterial evaluation.*Arid Zone Journal of Basic and Applied Research*. 1(1), 109-132.

[67]. Akter, M.J., Khatun, R., Khatune, N.A., Alam, A.K. & Rahman, M.A.A, (2022). In vitro antioxidant and free radical scavenging activity of the bark of Dillenia indica L. *Bangladesh Pharmaceutical Journal*. 25(1), 38-43.

[68]. Shah, S.S., Shah, D., Khan, I., Ahmad, S., Ali, U. & ur Rahman, A. (2020). Synthesis and antioxidant activities of Schiff bases and their complexes: An updated review. *Biological Interface Research and Applied Chemistry.* 10, 6936-6963.

[69]. Pal, S. & Pal, M. (2018). Isocoumarin, thiaisocoumarin and phosphaisocoumarin: natural occurrences, synthetic approaches and pharmaceutical applications.*Bioinorganic Chemistry*. 13(3), 1-14.

[70]. Lipinski, B. (2011). Hydroxyl radical and its scavengers in health and disease. *Oxidative Medicine and Cellular Longevity*.7(2), 1023-1037.

[71]. Gulcin, İ. & Alwasel, S.H. (2022). Metal ions, metal chelators and metal chelating assay as antioxidant method. *Processes*. 10(1), 132-146.